274 321

HEAT TRANSFER IN DISSOCIATED AIR BY A TWO-THICKNESS INTEGRAL METHOD
PART II: THE ZERO PRESSURE GRADIENT LAMINAR BOUNDARY LAYER

15 DECEMBER 1961

NOL

UNITED STATES NAVAL ORDNANCE LABORATORY, WHITE OAK, MARYLAND

Aeroballistics Research Report No. 149

HEAT TRANSFER IN DISSOCIATED AIR BY A TWO-THICKNESS INTEGRAL METHOD PART II: THE ZERO PRESSURE GRADIENT LAMINAR BOUNDARY LAYER

by

John O. Powers and Edgar Krahn

ABSTRACT: It has been previously shown (reference (a)), that the two-thickness integral method of determining boundary-layer characteristics provides reasonable results for stagnation-point flows even when the effects of equilibrium air dissociation are considered. This result implied that the method may have more general application and it therefore seemed advisable to explore additional characteristics of the method in order to further assess the extent of its applicability. The zero pressure gradient case, with its associated limiting cases, i.e., zero Mach number and zero heat transfer, has been used as a basis for this further evaluation primarily because of the availability for comparison of computations performed by "exact" methods. In general, it appears that of the profile representations considered, a two-parameter, sixth-degree velocity profile gives the most desirable results for a flat plate when used with the present method.

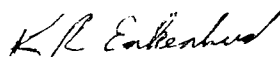PUBLISHED FEBRUARY 1962

U. S. NAVAL ORDANCE LABORATORY
WHITE OAK, MARYLAND

NOLTR 61-25   15 December 1961

W. D. COLEMAN
Captain, USN
Commander

K. R. ENKENHUS
By direction

ii

CONTENTS

ILLUSTRATIONS

TABLES

SYMBOLS

c_f	local skin-friction coefficient
C_f	mean skin-friction coefficient
E	total enthalpy thickness
$f(x,\bar{\eta})$	velocity ratio, u/U
$G(x,\bar{\eta}_H)$	total enthalpy ratio, $H/H_1 - 1$
h	static enthalpy
h_R	recovery enthalpy
H	total enthalpy
$H_i(\triangle *)$	polynomials used in equation (24) where $i = 1, \ldots 9$ (coefficients of polynomials given in Table I)
M	Mach number
p	static pressure
Pr	Prandtl number, including chemical contributions
q	heat-transfer rate
Re	Reynolds number based on length x
R	enthalpy recovery factor
S_T	Stanton number
T	temperature
u	x direction velocity component
U	velocity at the outer edge of the boundary layer.
v	y direction velocity component
$\tilde{v}$	η direction velocity component defined by equation (4)
x	co-ordinate along body in stream direction

y	co-ordinate normal to body surface
Y_1, Y_2, Y_3, Y_{11}	quantities define by equation (18a)
α_i	coefficients of thickness ratio equations (23) and (25) where $i = 0, 1, \ldots, 8$ (given in Table I)
β_i	coefficients given by equation (36) where $i = 1, 2$
δ	viscous boundary-layer thickness in x, η plane
$\delta*$	displacement thickness in x, η plane
Δ	thermal boundary-layer thickness in x, η plane
$\Delta*$	ratio of the thermal to viscous boundary-layer thickness in x, η plane
η	co-ordinate normal to body surface in transformed plane
$\bar{\eta}$	η/δ
$\bar{\eta}_H$	η/Δ
θ	momentum thickness in x, η plane
$\lambda_1(x)$	first velocity profile form factor defined by equation (11)
$\lambda_2(x)$	second velocity profile form factor defined by equation (11)
$\lambda_{H_0}(x), \lambda_{H_1}(x), \lambda_{H_2}(x)$	enthalpy profile form factors defined by equation (14)
$\bigwedge$	density thickness in x, η plane
μ	absolute viscosity
ξ	maximum (δ, Δ)
ρ	density
τ	shear stress
Subscripts	
w	wall conditions

vi

y	quantities in the physical plane
1	at outer edge of boundary layer
o	stagnation conditions at outer edge of boundary layer

HEAT TRANSFER IN DISSOCIATED AIR BY A
TWO-THICKNESS INTEGRAL METHOD
PART II: THE ZERO PRESSURE GRADIENT
LAMINAR BOUNDARY LAYER

INTRODUCTION

1. The two-thickness integral method of computing laminar boundary-layer characteristics at the stagnation point of bodies including the effects of dissociated air in equilibrium has been presented in reference (a). From that investigation, it appeared that the method may have more general application and, accordingly, it was considered desirable to investigate additional characteristics of the method. The procedure presented was based on an extension of the Karman-Pohlhausen method as reported by Morris and Smith (reference (b)), and had been modified to include the latest information on the thermodynamic and transport properties of air as determined by members of the Thermodynamic Section, National Bureau of Standards (NBS). The further investigation has been conducted on the zero-pressure gradient boundary layer and the results have been compared with the results of "exact" methods (references (c), (d), (e), and (f)).

2. Van Driest (reference (d)) and Klunker and McLean (reference (e)), both consider the temperature variation of the fluid properties but do not perform calculations for temperatures at which air becomes dissociated. The property values used in references (d) and (e) were different, hence, discrepancies between these results may be attributed primarily to this difference. The method of solution of the basic differential equations was similar in that a transformation was used to obtain an equation in integral form which in turn was solved by the method of successive approximations. The transformations were different, however, because Van Driest used Crocco's procedure which results in velocity as the independent variable whereas Klunker and McLean used the procedure of Schuh which yields normal distance as the independent variable.

3. The recent work of Wilson (reference (f)) which is based on the Crocco procedure, permits comparison with the two-thickness integral method in temperature regions where dissociation affects the property values. Wilson used the most current NBS thermodynamic and transport data available at the time of his investigation; however, since the amount of transport property data was limited in the dissociation region, it was necessary for him to devise an interpolation scheme which produced reliable results over a wide range of stream-to-reference-density ratios. Since the completion of the

1

reference (f) investigation, the NBS (reference (g)) has generated new transport property data in the temperature range between 2700°R and 6000°R. The two sets of property data compare very favorably with the largest discrepancy (approximately five percent), appearing in the Prandtl number at 2800°R. The reference (g) data have been incorporated herein and the interpolation scheme of reference (f) has been used for viscosity determination at temperatures above 6000°R.

4. In Part I of this investigation (i.e., "Stagnation Point Heat Transfer," reference (a)), a one parameter, fourth-degree polynomial velocity-profile representation was used because of its known suitability for stagnation point flows. When applied to general cases, this representation results in a limitation because of the single parameter, namely, that its absolute value cannot exceed 12. Such a limitation is characteristic of methods based on the Pohlhausen procedure. Accordingly, in the Part II investigation reported herein a two-parameter velocity-profile representation was used in an attempt to extend the range of applicability of the method. In addition, fourth-, fifth-, and sixth-degree velocity polynomials have been used, and total as well as static enthalpy profiles, both of the sixth-degree, were investigated. While altering the velocity profile representation avoids some limitations, other limitations are introduced. The zero pressure-gradient case has the advantage of presenting an opportunity to explore some of these limitations without introducing excessive complexity.

ANALYSIS

5. The complete equations of motion including pressure gradient for the flow of a real-gas compressible fluid are given in reference (a). For a two-dimensional, zero pressure-gradient boundary layer the equations become:

$$\frac{\partial}{\partial x}(\rho u) + \frac{\partial}{\partial y}(\rho v) = 0 \qquad \text{(continuity)} \quad (1)$$

$$\rho u \frac{\partial u}{\partial x} + \rho v \frac{\partial u}{\partial y} = \frac{\partial}{\partial y}\left(\mu \frac{\partial u}{\partial y}\right) \qquad \text{(momentum)} \quad (2)$$

$$\rho u \frac{\partial h}{\partial x} + \rho v \frac{\partial h}{\partial y} = \mu\left(\frac{\partial u}{\partial y}\right)^2 + \frac{\partial}{\partial y}\left(\frac{\mu}{P_r}\frac{\partial h}{\partial y}\right) \qquad \text{(energy)} \quad (3)$$

2

It is noted that the Prandtl number used in the energy equation includes contributions of both the conductive and ordinary diffusive energy fluxes for air in equilibrium dissociation.

6. As in the reference (a) development, the partial differential equations (1), (2), and (3) are initially transformed from the x, y plane to the x, η plane by the Dorodnitsyn transformation in the form

$$\eta = \int_0^y \frac{\rho}{\rho_0} \cdot dy$$

As a result of this transformation, the continuity, momentum, and energy equations become:

$$\frac{\partial u}{\partial x} + \frac{\partial \tilde{v}}{\partial \eta} = 0 \qquad \text{WHERE} \qquad \tilde{v} = u \frac{\partial \eta}{\partial x} + \frac{\rho v}{\rho_0} \qquad (4)$$

$$u \frac{\partial u}{\partial x} + \tilde{v} \frac{\partial u}{\partial \eta} = \frac{1}{\rho_0^2} \frac{\partial}{\partial \eta} \left(\rho \mu \frac{\partial u}{\partial \eta} \right) \qquad (5)$$

$$u \frac{\partial h}{\partial x} + \tilde{v} \frac{\partial h}{\partial \eta} = \frac{\rho \mu}{\rho_0^2} \left(\frac{\partial u}{\partial \eta} \right)^2 + \frac{1}{\rho_0^2} \frac{\partial}{\partial \eta} \left(\frac{\rho \mu}{P} \frac{\partial h}{\partial \eta} \right) \qquad (6)$$

7. When it is assumed that the total enthalpy,

$$H_0 = h_1 + \frac{U^2}{2}$$

at the edge of the boundary layer is constant and equations (5) and (6) are integrated from the wall to the outer edge of the boundary layer, the result is:

$$\frac{d\Theta}{dx} = \frac{\tau_w}{\rho_0 U^2} \qquad (7)$$

and

$$\frac{dE}{dx} = \frac{q_w}{\rho_0 U H_0} \qquad (8)$$

3

where q_w and τ_w are respectively the heat transfer and shear stress at the wall. The corresponding integral equations for the pressure gradient case are given in reference (a). The boundary-layer momentum thickness, θ, and total enthalpy thickness, E, are defined in the transformed plane as:

$$\theta = \int_0^\xi \frac{u}{U}\left(1 - \frac{u}{U}\right) d\eta$$

$$\xi = MAX(\delta, \Delta) \qquad (9a)$$

$$E = \int_0^\xi \frac{u}{U}\left(\frac{H}{H_0} - 1\right) d\eta$$

where δ and Δ are the values of η at the outer edge of the viscous and thermal boundary layers, respectively. The displacement thickness, δ^*, and the density thickness, Λ which supply additional information but are not essential for the solution of the system of equations, are defined as:

$$\delta^* = \int_0^\xi \left(1 - \frac{u}{U}\right) d\eta$$

$$\qquad (9b)$$

$$\Lambda = \int_0^\xi \left(\frac{\rho_1}{\rho} - 1\right) d\eta$$

The inverse transformations of these thicknesses, including the viscous and thermal thicknesses, are:

$$\theta_y = \int_0^{\xi_y} \frac{\rho u}{\rho_1 U}\left(1 - \frac{u}{U}\right) dy = \frac{\rho_0}{\rho_1}\theta$$

$$E_y = \int_0^\xi \frac{\rho u}{\rho U}\left(\frac{H}{H_1} - 1\right) dy = \frac{\rho_0}{\rho_1} E$$

$$\delta_y^* = \int_0^{\xi_y} \left(1 - \frac{\rho u}{\rho U}\right) dy = \frac{\rho_0}{\rho_1}\left[\Lambda + \delta^*\right] \qquad (10)$$

$$\Lambda_y = \int_0^{\xi_y} \left(\frac{\rho_1}{\rho} - 1\right) dy = \rho_0 \int_0^\Delta \left(\frac{\rho_1 - \rho}{\rho^2}\right) d\eta$$

$$\delta_y = \frac{\rho_0}{\rho_1}\left[\Lambda + \delta\right]$$

$$\Delta_y = \frac{\rho_0}{\rho_1}\left[\Delta + \int_0^\Delta \left(\frac{\rho_1}{\rho} - 1\right) d\eta\right]$$

where quantities in the physical plane are indicated by the subscript y and ξ is the maximum of δ or Δ.

PROFILE REPRESENTATION

8. The foregoing development differs from the Part I (reference (a)) development only in the fact that the pressure gradient terms have been omitted for the basic equations. In the Part II investigations, an attempt was made to extend the range of applicability of the method and accordingly, a two-parameter velocity-profile representation was used instead of the one-parameter representation as used in Part I. It was also considered desirable to utilize fourth-, fifth-, and sixth-degree polynomials for the velocity profiles to evaluate the relative advantages of each by comparing the results with other methods. Parametrically, the velocity profiles are presented in the form:

$$f(x, \bar{\eta}) = \frac{u}{U} = f_0(\bar{\eta}) + \lambda_1(x) f_1(\bar{\eta}) + \lambda_2(x) f_2(\bar{\eta}) \tag{11}$$

where $\bar{\eta} = \eta/\delta$ and the parameters λ_1 and λ_2 are defined by equation (17). In forming the profiles, it was considered desirable to utilize as many wall boundary conditions as practical since the phenomena of interest occur primarily at the wall. The boundary conditions used varied with the degree of the polynomial and are the following:

$f_0(0) = 0$	$f_1(0) = 0$	$f_2(0) = 0$
$\ddot{f}_0(0) = 0$	$\ddot{f}_1(0) = -1$	$\ddot{f}_2(0) = 0$
$\dddot{f}_0(0) = 0$	$\dddot{f}_1(0) = 0$	$\dddot{f}_2(0) = -1$
$f_0(1) = 1$	$f_1(1) = 0$	$f_2(1) = 0$ (12)
$\dot{f}_0(1) = 0$	$\dot{f}_1(1) = 0$	$\dot{f}_2(1) = 0$
$\ddot{f}_0(1) = 0$	$\ddot{f}_1(1) = 0$	$\ddot{f}_2(1) = 0$ (used only for fifth- and sixth-degree polynomials)
$\dddot{f}_0(1) = 0$	$\dddot{f}_1(1) = 0$	$\dddot{f}_2(1) = 0$ (used only for sixth-degree polynomials)

where the dot denotes differentiation with respect to $\bar{\eta}$. Physically, these conditions correspond to the zero slip condition at the wall, satisfy the momentum equation at the wall through the second and third derivatives of the velocity profiles, and insure a smooth transition to the external inviscid flow. As

a result of the use of these boundary conditions, the polynomials become:

$$f_o = \begin{cases} 1/3 \ (4\bar{\eta} - \bar{\eta}^4) \text{ or} \\ 1/3 \ (5\bar{\eta} - 5\bar{\eta}^4 + 3\bar{\eta}^5) \text{ or} \\ 2\bar{\eta} - 5\bar{\eta}^4 + 6\bar{\eta}^5 - 2\bar{\eta}^6 \end{cases}$$

$$f_1 = \begin{cases} 1/6 \ (2\bar{\eta} - 3\bar{\eta}^2 + \bar{\eta}^4) \text{ or} \\ 1/4 \ (\bar{\eta} - 2\bar{\eta}^2 + 2\bar{\eta}^4 - \bar{\eta}^5) \text{ or} \\ 1/10 \ (2\bar{\eta} - 5\bar{\eta}^2 + 10\bar{\eta}^4 - 10\bar{\eta}^5 + 3\bar{\eta}^6) \end{cases} \tag{13}$$

$$f_2 = \begin{cases} 1/18 \ (\bar{\eta} - 3\bar{\eta}^3 + 2\bar{\eta}^4) \text{ or} \\ 1/36 \ (\bar{\eta} - 6\bar{\eta}^3 + 8\bar{\eta}^4 - 3\bar{\eta}^5) \text{ or} \\ 1/60 \ (\bar{\eta} - 10\bar{\eta}^3 + 20\bar{\eta}^4 - 15\bar{\eta}^5 + 4\bar{\eta}^6) \end{cases}$$

9. Total enthalpy profiles are used primarily herein whereas in Part I (reference (a)) static enthalpy profiles were used. While the choice of total enthalpy profiles results in some simplification of the mathematical expressions involved it does impose a limitation on the method which is discussed in Paragraphs 20 through 22. The form of the total enthalpy profile is the same as that of the static enthalpy profile; namely:

$$G(x, \bar{\eta}_H) = \frac{H}{H_1} - 1 = \lambda_{H_o}(x) G_o(\bar{\eta}_H) + \lambda_{H_1}(x) G_1(\bar{\eta}_H) + \lambda_{H_2}(x) G_2(\bar{\eta}_H) \tag{14}$$

where $\bar{\eta}_H = \eta/\Delta$ and λ_{H_o}, λ_{H_1}, λ_{H_2}, are defined by equations 17 and 18. The physical boundary conditions are at $y = 0$, $H = H_w$, and the second and third derivatives of the enthalpy profiles satisfy the energy equation, and at $y = \infty$, $H = H_1$ and the first three derivatives of the enthalpy profiles are zero. The corresponding transformed plane boundary conditions and, hence, the polynomials, are therefore:

$G_o(0) = 1$	$G_1(0) = 0,$	$G_2(0) = 0$
$\ddot{G}_o(0) = 0$	$\ddot{G}_1(0) = -1$	$\ddot{G}_2(0) = 0$
$\dddot{G}_o(0) = 0$	$\dddot{G}_1(0) = 0$	$\dddot{G}_2(0) = 1$
$G_o(1) = 0$	$G_1(1) = 0$	$G_2(1) = 0$
$\dot{G}_o(1) = 0$	$\dot{G}_1(1) = 0$	$\dot{G}_2(1) = 0$
$\ddot{G}_o(1) = 0$	$\ddot{G}_1(1) = 0$	$\ddot{G}_2(1) = 0$
$\dddot{G}_o(1) = 0$	$\dddot{G}_1(1) = 0$	$\ddot{G}_2(1) = 0$

6

$$G_O \, (\bar{\eta}_H) = 1 - 2\bar{\eta}_H + 5\bar{\eta}_H^4 - 6\bar{\eta}_H^5 + 2\bar{\eta}_H^6$$

$$G_1 \, (\bar{\eta}_H) = 1/10 \, (2\bar{\eta}_H - 5\bar{\eta}_H^2 + 10\bar{\eta}_H^4 - 10\bar{\eta}_H^5 + 3\bar{\eta}_H^6) \quad (16)$$

$$G_2 \, (\bar{\eta}_H) = 1/60 \, (-\bar{\eta}_H + 10\bar{\eta}_H^3 - 20\bar{\eta}_H^4 + 15\bar{\eta}_H^5 - 4\bar{\eta}_H^6)$$

10. The equations (11), (12), (14), and (15) result in the following definitions of the profile parameters

$$\lambda_1(X) = \frac{-\partial^2(u/U)}{\partial \bar{\eta}^2}\bigg|_w$$

$$\lambda_2(X) = \frac{-\partial^3(u/U)}{\partial \bar{\eta}^3}\bigg|_w$$

$$\lambda_{H_0}(X) = \frac{HW}{H_0} - 1$$

$$\lambda_{H_1}(X) = \frac{-\partial^2(H/H_0)}{\partial \bar{\eta}_H^2}\bigg|_w \quad (17)$$

$$\lambda_{H_2}(X) = \frac{\partial^3(H/H_0)}{\partial \bar{\eta}_H^3}\bigg|_w$$

The expressions for the profile parameters, or form factors, are then derived for the zero pressure gradient case by direct differentiation of the transformed momentum and energy equations (equations (5) and (6)). These expressions are:

$$\lambda_1(X) = \frac{\dot{G}(X,0)\,\dot{f}(X,0)\,H_0\,Y_1}{\Delta^*}$$

$$\lambda_2(X) = \dot{f}(X,0)\left[\frac{\dot{G}(X,0)\,H_0}{\Delta^*}\right]^2 \left[Y_1 - Y_1^2\,Y_1\,Y_2\right] - Pr_w\,U^2\,\dot{f}(X,0)^3\,Y_1$$

$$\lambda_{H_1}(X) = H_0\,Y_2\,\dot{G}(X,0)^2 - \frac{(1-Pr_w)[U\Delta^*\dot{f}(X,0)]^2}{H_0} \quad (18a)$$

$$\lambda_{H_2}(X) = \dot{G}(X,0)[U\Delta^*\dot{f}(X,0)]^2\,[(Pr_w - 3)Y_1 + 3\,Pr_w\,Y_2]$$

$$+ \dot{G}(X,0)^3\,H_0^2[2\,Y_2^2 - Y_3] + \frac{(\rho_0\,\delta)^2\Delta^{*3}U\dot{f}(X,0)Pr_w}{\rho_w\,\mu_w\,H_1}\,\frac{\partial h_w}{\partial X}$$

where the Y's, which are determined from real-gas property values and hence are functions of pressure and enthalpy, are defined as:

7

$$Y_1 = \frac{\partial \ln \rho\mu}{\partial h}$$

$$Y_2 = \frac{\partial \ln (\rho\mu/P_r)}{\partial h}$$

(18b)

$$Y_3 = \frac{\partial^2 \ln (\rho\mu/P_r)}{\partial h^2}$$

$$Y_{11} = \frac{\partial^2 \ln \rho\mu}{\partial h^2}$$

and Δ^* is the ratio of the thermal and viscous thicknesses, i.e., $\Delta^* = \dfrac{\Delta}{\delta}$.

THERMODYNAMIC AND TRANSPORT PROPERTIES

11. Since the real-gas characteristics of the present method are dependent on the air property values, only the most recent data on the properties of air in equilibrium dissociation have been used. These values have been generated by the Thermodynamics Section of the National Bureau of Standards and were obtained from references (g), (h), and (i). The density, as used in the computations, was taken inversely proportional to the temperature at constant pressure for temperatures up to 2520°R. For temperatures greater than 2520°R, the density was then determined as a function of pressure and enthalpy by curve fits to the data of reference (h) as developed by Schmid, reference (j). In addition to an accurate knowledge of the density it was necessary to have reliable values of the viscosity and Prandtl number so that the derivatives of the quantities $\ln\rho\mu$ and $\ln\rho\mu/Pr$ could be formed. The values given in reference (i) were considered adequate for temperatures below 2700°R; however, for temperatures between 2700°R and 6000°R, new constant-pressure transport-property tables were generated by Klein, reference (g), presenting the data at small temperature increments to facilitate differentiation. Since the derivatives of the property values are needed only at wall temperatures, the tables of reference (g) were terminated at 6000°R which is considered more than adequate for practical wall temperatures. The only transport property information needed at higher temperatures was the viscosity for the computation of the stream Reynolds numbers. Viscosities at temperatures above 6000°R were determined by the interpolation scheme of reference (f).

8

12. The need for accurate determination of the property derivatives (i.e., equation (18b)) is apparent from their contribution to the velocity and enthalpy form factors; equation (18a). In fact, under some conditions, inaccuracies in these derivatives could result in the loss of solutions as will be discussed in the section on limitations. In an effort to obtain maximum accuracy of the derivatives, the data of references (g) and (i) were smoothed by the numerical procedures described in reference (k), numerically differentiated by the methods outlined in Chapter IV of reference (1) and re-smoothed to obtain the first derivative. This procedure was repeated, using the results of the first differentiation, to obtain the second derivative. It was then necessary to make slight additional adjustments to assure the proper agreement between the derivatives and the original quantities. The values used are presented in Figure 1.

SOLUTION OF THE SYSTEM OF EQUATIONS

13. The basic system of equations to be solved consists of equations (7), (8), (9a), (11), (14), and (18a). Examination of the equations indicates that a solution may readily be obtained if the profile parameters are assumed to be independent of x (also H_0, h_w, U, and P are constant). This is physically equivalent to the assumption of similar profiles which is consistent with other zero pressure gradient analyses (e.g., references (c), (d), (e), and (f)).

14. As a result of the above assumptions, equations (7) and (8) may be integrated. Using the definitions of shear stress and heat transfer as:

$$\tau_w = \frac{(\rho \mu f)_w \, U}{\rho_0 \, \delta} \tag{19}$$

$$\dot{q}_w = -\frac{(\rho \mu \dot{G})_w \, H_0}{\rho_0 \, Pr_w \, \Delta} \tag{20}$$

where the subscript w refers to quantities at the wall, the integration gives, (for $\theta = E = 0$ at $x = 0$):

$$\theta^2 = \frac{2(\rho \mu f)_w}{\rho_0^2 \, U} \, \frac{\theta}{\delta} \, x \tag{21}$$

9

$$E^{-2} = - \frac{2(\rho \mu \dot{G})_w}{\rho_o^2 P_w U} \frac{E}{\Delta} x \tag{22}$$

15. We now develop equations (9a) so that the ratios θ/δ and E/Δ may be expressed in terms of the profile parameters and the boundary-layer thickness ratio $\Delta*$. This is accomplished by inserting the polynomials for the velocity and total enthalpy in equations (9a) and performing the indicated integration. The results are expressed in terms α_i's and $H_i(\Delta*)$ where the α_i's are constants the $H_i(\Delta*)$'s are polynomials in $\Delta*$. The constants and the coefficients for the polynomials are presented in Table I for fourth-, fifth-, and sixth-degree velocity profiles and for $\Delta*$ greater or less than one. The required ratios are:

$$\frac{\theta}{\delta} = \alpha_0 - \alpha_3 + (\alpha_1 - 2\alpha_6)\lambda_1 + (\alpha_2 - 2\alpha_7)\lambda_2$$
$$- \alpha_4 \lambda_1^2 - \alpha_5 \lambda_2^2 - 2\alpha_8 \lambda_1 \lambda_2 \tag{23}$$

$$\frac{E}{\Delta} = H_1(\Delta*)\lambda_{H_0} + H_2(\Delta*)\lambda_{H_1} + H_3(\Delta*)\lambda_{H_2} + H_4(\Delta*)\lambda_1\lambda_{H_0}$$
$$+ H_5(\Delta*)\lambda_1\lambda_{H_1} + H_6(\Delta*)\lambda_1\lambda_{H_2} + H_7(\Delta*)\lambda_2\lambda_{H_0} \tag{24}$$
$$H_8(\Delta*)\lambda_2\lambda_{H_1} + H_9(\Delta*)\lambda_2\lambda_{H_2}$$

The additional quantity:

$$\frac{\delta*}{\delta} = 1 - \alpha_0 - \alpha_1\lambda_1 - \alpha_2\lambda_2 \tag{25}$$

is developed from equation (9b) in a similar manner; however, the values of Λ/Δ must be determined by direct integration after the values of λ_{H_1} and λ_{H_2} are known.

16. If equations (11) and (14) are differentiated with respect to $\bar{\eta}$ and $\bar{\eta}_H$ and given in terms of the wall values (i.e., $\bar{\eta} = \bar{\eta}_H = 0$) we have

$$\dot{f}_w = \dot{f}_0(0) + \lambda \dot{f}_1(0) + \lambda_2 \dot{f}_2(0) \qquad (26)$$

$$\dot{G}_w = \lambda_{H_0} \dot{G}_0(0) + \lambda_{H_1} \dot{G}_1(0) + \lambda_{H_2} \dot{G}_2(0) \qquad (27)$$

These two equations, equations (21) through (24), and the equation (18) now independent of x, constitute the systems of equations which were actually solved.

17. The method of solution was iterative and consisted of the following steps. First values of λ_1 and λ_2 were assumed, $\dot{f}_w$ was then computed from equation (26) and next $\dot{G}_w/\triangle*$, $\lambda_{H_1}/\triangle*^2$ and $\lambda_{H_2}/\triangle*^3$ were determined from the first, third, and fourth equation (18). These quantities were inserted in equation (27) and a cubic in $\triangle*$ was formed. The root of the cubic to be used was decided on the basis of physical reasoning and then $\dot{G}_w$, λ_{H_1}, and λ_{H_2} were computed. Now all quantities of interest were available and it was necessary to check the assumed values of λ_1 and λ_2. The second equation (18) gave a direct check on λ_2; however, it was necessary to combine equations (21) through (24) to check λ_1 in terms of the computed $\dot{G}_w$. When the differences between the computed quantities and the quantities as determined by the checking equations was less than 0.001 percent, the solution was considered satisfactory. If the checking equation was not satisfied, λ_1 and λ_2 were incremented by both positive and negative quantities and the iteration process was repeated until satisfactory results were achieved.

18. After the system of equations was solved, the values of $\delta*$ and Λ were obtained from equation (25) and equation (9b), respectively. Next, the inverse transformations, equations (10), were applied to obtain the boundary-layer thicknesses in the physical plane as a function of the square root of x;

i.e., $\delta_y/\sqrt{x}$ or $\frac{\delta_y}{x}\sqrt{Re}$ is constant. The shear stress and heat

transfer at the wall may now be expressed as function of $\sqrt{x}$ by equations (19) and (20). If the local skin-friction coefficient, c_f, is desired it may be derived from equation (21) as:

$$ C_f \sqrt{R_{e_{l,x}}} = \sqrt{2\dot{f}_w \frac{\theta}{\delta} \frac{\rho_w \mu_w}{\rho_l \mu_l}} = \frac{1}{2} C_f \sqrt{R_{e_{l,x}}} \qquad (28) $$

where θ/δ is given by equation (23) and C_f is the mean friction coefficient. Similarly, if a Stanton number,

$$ St = \frac{\dot{t}_w}{v_l U_l (h_R - h_w)} $$

is desired, equation (29) may be developed to give:

$$ St \sqrt{R_{e_{l,x}}} = \sqrt{\frac{-\dot{G}_w}{2 P_{r_w}} \frac{\rho_w \mu_w}{\rho_l \mu_l} \frac{E}{\Delta}} \frac{H_o}{(h_R - h_w)} \qquad (29) $$

where E/Δ is given by equation (24) and h_R is the recovery enthalpy.

19. When computing the recovery enthalpy as defined by the relations:

$$ h_R = h_l + R \frac{U_l^2}{2} \qquad (30) $$

and

$$ R = \frac{h_R - h_l}{H_o - h_l} . \qquad (31) $$

some investigators, (e.g., references (d) and (e)) have found that R is a function of Mach number and wall-to-stream temperature ratio. The heat-transfer results presented herein were calculated using total enthalpy profiles and are based on a unity recovery factor to avoid ambiguity as to the choice of recovery factor used in the computations. The heat-transfer results of reference (f) have also been adjusted to a unity recovery factor. For purposes of comparison some recovery factors have been computed for the case of an insulated wall using only static enthalpy profiles. Difficulties, discussed in Paragraph 21, were encountered when the total enthalpy profiles were used to derive the insulated wall recovery

factor. The recovery factor for the static enthalpy profiles
is:

$$R = 0.2 \, Pr_w \, (\Delta^* \dot{f}_w)^2 \tag{32}$$

where $\dot{f}_w$ is found from equation (26) with λ_1 equal to zero.
The quantity Δ^* is found from a form of equation (24) derived
with a static enthalpy profile and with E/Δ, λ_1, and λ_{H_2}
equal to zero.

LIMITATIONS OF METHOD

20. The one-parameter velocity profile representation, as
described in Part I, reference (a), results in a limitation
to the range of applicability of the present method. This
limitation occurs because under most physically realistic
flow conditions the absolute value of the profile parameter
cannot exceed 12. Physically, the existence of profile param-
eters less than minus 12 indicates that flow separation would
occur and if the parameter exceeded plus 12 it indicates that
velocity overshoot occurs within the boundary layer. While
the latter case is possible under some conditions of heat
transfer it is normally not probable for cases with heat
transfer to the surface and, therefore, is a limitation on
physical grounds. Actually the significant root of the equation
for the velocity profile parameter became imaginary in the one
parameter method after its value reached 12. The limitations
of flow separation and velocity overshoot are general and also
apply to the two-parameter velocity profile representation.
In this case, the limiting values of λ_1 and λ_2 are found by
equating the derivative of the velocity profile to zero, i.e.,
$\dot{f}(x,\bar{\eta}) = 0$, which gives a linear relation between the variables
λ_1 and λ_2 for a fixed value of $\bar{\eta}$. Then $\bar{\eta}$ is eliminated
from the family of such linear relations yielding an envelope
whose interior represents the allowable values of λ_1 and λ_2.
The envelopes vary with the degree of the polynomial and are
presented in Figure 2 for fourth-, fifth-, and sixth-degree
polynomials. It is noted that the higher degree polynomial
yields a larger envelope. While these envelopes were not
exceeded for any of the flat-plate cases presented, they are
useful as an indication of the validity of solutions obtained
in more general cases such as with pressure gradient.

21. In a somewhat similar manner, the choice of sixth-degree
total-enthalpy profiles imposes a limitation on the values of
the wall heat transfer which may be obtained. This limitation
results in an inability to represent the zero heat-transfer

total-enthalpy profile and implies that calculations near zero heat transfer may be suspect. In this case, λ_{H2} is zero and $G(\bar{\eta}_H) = 0$ yields a condition when $\bar{\eta}_H = 0$ such that no further values of $\dot{G}(\bar{\eta}_H) = 0$ are possible for $\bar{\eta}_H$ between zero and one. An additional zero derivative, however, is necessary in the $\bar{\eta}_H$ range to represent properly the zero heat-transfer total-enthalpy profile. Fortunately, this limitation does not exist when either the pressure gradient or wall enthalpy gradient is non-zero.

22. Another limit which is applicable to the zero pressure gradient case is brought about by unfavorable combinations of property values (i.e., equation (18b)), and flow conditions. By combining the first two equations of (18a) with equation (26), a quadratic equation may be formed in terms of λ_1. When the resulting equation is solved for λ_1 the discriminant may become negative and, hence, lead to complex values of λ_1. This limit, which varies with the degree of the velocity polynomial, is not violated if the following inequalities are satisfied.

Fourth degree $-\beta_1\frac{\beta_2}{2} \dot{f}_w^{\,3} - 9\dot{f}_w(2\beta_1-1)+24\beta_1 \geqq 0$ (33)

Fifth degree $-\beta_1\frac{\beta_2}{2} \dot{f}_w^{\,3} - \frac{9}{4}\dot{f}_w(16\beta_1-9)+60\beta_1 \geqq 0$ (34)

Sixth degree $-\beta_1\frac{\beta_2}{2}\dot{f}_w^{\,3} - 12\dot{f}_w(5\beta_1-3)+120\beta_1 \geqq 0$ (35)

where $\beta_1 = \frac{Y_2}{Y_1} - \frac{Y_{11}}{Y_1^2} +1$ AND $\beta_2 = 2 P_{r_w}(H_o-h_1)Y_1$ (36)

Since β_1 and $\beta_2/(H_o - h_1)$ are functions of wall temperature and pressure it is difficult to generalize with respect to

14

the above inequalities. Figure 3 has therefore been plotted for 0.1 atmosphere pressure and presents the value of the left-hand member of the inequality (designated as G (β_1, β_2)

as a function of h_w/RT_0, where $RT_0 = 33.7098$ BTU/lb, for constant values of $\dot{f}_w$ and $H_0 - h_1$. Since $\dot{f}_w$ must be positive and generally lies between one and two, this presentation gives a qualitative guide to the combination of conditions which should fail to give solutions. The curves, which are exceedingly irregular because of the real-gas properties used, i.e., Figures 1c and 1d, indicate that the criterion should be examined on a per case basis. It was also noted that changes in Y_{11} which were smaller than the expected accuracy of the

numerically determined second derivatives could change a case from violating to satisfying the criterion. From this it must be concluded that still further accuracy is needed in determining the property derivatives, i.e., the equation (18a) quantities. Figure 3 shows in addition that excessively large values of $(H_0 - h_1)$ and small values of f_2 have a greater

probability of failing to yield solutions. One may also observe that for a perfect gas with constant Prandtl number and constant coefficient of specific heat and viscosity described by the Sutherland's law the value of f_1 is always positive and

hence, the criterion is satisfied in almost all practical cases.

RESULTS AND DISCUSSION

23. It was pointed out in the section on limitations* that the use of total-enthalpy profiles precluded investigation of the zero heat transfer (i.e., insulated wall case). In order to obtain a skin friction Mach number relationship for zero heat transfer, a limited number of computations were made with static enthalpy profiles and sixth-degree velocity profiles. The results, in terms of $C_f\sqrt{R}$ vs. M_1, are presented in Figure 4. In Figure 5 the corresponding insulated wall enthalpy recovery factor is presented. These computations were made using equation (32) and also by using the square root of the Prandtl number taken at the derived wall temperature in zero heat transfer. The present values are compared with those of references (d) and (e). From Figure 4a it is seen that the agreement in $C_f\sqrt{R}$ is reasonable at

---

* Because of the indicated limitations all results are given in the figures with symbols used to represent actual computed values. In some cases the curves have been faired through regions where solutions are not attainable.

all stream Mach numbers with slight discrepancies occurring
at Mach number near one. Correspondingly good agreement is
noted in Figure 5 for the insulated wall enthalpy recovery
factor where the greatest discrepancy between the methods
is in the order of five percent. As has been noted by other
investigators, the enthalpy recovery factor curve varies
closely as the square root of the wall Prandtl number. These
results indicate that if investigations are to be conducted
by the two parameter integral method, use of static enthalpy
profiles should give reasonable results for cases near zero
heat transfer, whereas, the use of total-enthalpy profiles
would fail to give satisfactory values.

24. Since the case of equal wall and stream temperatures
reduces to the zero heat-transfer case at zero Mach number
it was considered a desirable case for comparing the results
obtained by using velocity profiles of varying degree. Fourth-,
fifth-, and sixth-degree velocity polynomials were used as
well as a sixth-degree total enthalpy presentation. The
computed values of $c_f \sqrt{Re}$ are shown in Figure 4 as a function
of Mach number. As might be expected the higher degree pro-
file polynomials give the better agreement with the less
approximate methods. The sixth-degree presentation is within
less than one percent of the Blasius value at zero Mach number.
As the Mach number is increased, however, the results of the
methods (i.e., references (c) and (e), and the present method)
diverge considerably, differing by as much as 20 percent at
Mach number 20. As will be seen later, this difference is not
typical of most cases but may be interpreted as an indication
of a difficiency in the present method when computing cases
where the wall-to-stream static enthalpy ratio is in the order
of one and the Mach number is large.

25. The methods of references (c), (d), and (e) do not include
the effects of air dissociation on the thermodynamic and trans-
port properties and, hence, comparisons with the two-thickness
integral method in regions where dissociation is present are
at best qualitative. The recent work of Wilson, reference
(f), does present an opportunity for quantitative comparison
in the dissociation region. Following Wilson the skin friction
is presented in Figures 6 and 7 as a function of wall-to-stream
static enthalpy ratio for constant values of the parameter
$U^2/2h_1$ at stream enthalpies of 93.24 and 466.3 BTU/lb (i.e.,
3000 and 15,000 BTU/slug). Both fourth- and sixth-degree
velocity polynomials and total-enthalpy profiles were used to
obtain the results which are presented and again the agreement
is considerably more favorable when the sixth-degree polynomials
are used. The results obtained with the sixth-degree velocity
profiles are generally within approximately five percent of
the reference (f) values with the notable exception of the

region of low wall-to-stream enthalpy ratio. The reason for
this difference is not clear at present but is believed to
be associated with the occurrence of an inflection point in
the transformed plane velocity profiles which is uniquely
fixed in $\bar{\eta}$ by the polynomial approximation. The transformed
plane inflection point itself appears to be necessary to
accommodate the large static enthalpy gradients which are
present in these highly cooled wall cases.

26.   In Figure 8 the present results are compared with those
of reference (f) on the basis of a modified Reynolds analogy
parameter,

$$\frac{2 St\ Pr_w^{2/3}}{C_f} = 1$$

The Stanton number for the present results were determined
using a unity recovery factor. It was therefore necessary
to alter the reference (f) results to include a unity recovery
factor so that a common basis of comparison was achieved.
Here again, the sixth-degree velocity profiles appear to give
a better representation of the physical picture. With respect
to heat transfer, however, Figure 9 shows good agreement
between the two methods which implies that the differences
indicated in the modified Reynolds analogy factor are due
to the previously discussed differences in the skin friction.
With respect to the two-thickness integral method, it appears
that the use of either the fourth- or sixth-degree velocity
profile representation give essentially identical values of
the heat transfer.

27.   A limited investigation of the effect of pressure level
on the skin-friction coefficients and modified Reynolds
analogy factor was conducted. The results presented in
Figures 10 and 11 do not show any striking features except
possibly a larger effect of wall-to-stream enthalpy ratio
at the larger pressure levels.

28.   As a final comparison between the results of the reference
(f), and the present method, velocity and static enthalpy
profiles in the physical plane are presented in Figure 12.
The case presented is for a wall-to-stream enthalpy ratio of
one and as previously discussed (Paragraph 25) represents the
area of greatest divergence between the two methods. It is
interesting to note that, in the lower half of the boundary
layer, the profiles are quite similar. While it is difficult
to generalize, this may indicate that quantities such as heat
transfer and skin friction which are dependent on derivatives
of the profiles at the wall could be reasonably well repre-
sented.

CONCLUSIONS

29. In general, it may be concluded that the two-thickness integral method utilizing a sixth-degree polynomial velocity profile representation gives reasonable results when compared with the "exact" methods.

30. The present investigation has also revealed limitations of the two-parameter polynomial-approximation procedure most of which must be examined on a per case basis. Among the limitations are the following:

    a. The possibility of loss of solutions due to unfavorable combinations of thermodynamic and transport property derivatives.

    b. The failure of total enthalpy profile polynomials in cases of zero, or near zero, heat transfer.

REFERENCES

(a) Powers, J. O. and Krahn, E., "Heat Transfer in Dissociated Air by a Two-Thickness Integral Method. Part I: Stagnation Point Heat Transfer," NAVORD Report 6673, 24 September 1959

(b) Morris, D. M. and Smith, J. W., "The Compressible Laminar Boundary Layer with Arbitrary Pressure and Surface Temperature Gradients," Jour. Aero. Sci., Vol. 20, No. 12, December 1953

(c) Van Driest, E. R., "Investigation of Laminar Boundary Layer in Compressible Fluids Using the Crocco Method," NACA TN 2597, January 1952

(d) Van Driest, E. R., "High Speed Aerodynamics and Jet Propulsion," Volume 5, Section F, pp. 339-370, Princeton Press

(e) Klunker, E. B. and McLean, F. E., "Effect of Thermal Properties on Laminar Boundary-Layer Characteristics," NACA TN 2916, March 1953

(f) Wilson, R. E., "Real Gas Laminar Boundary Layer: Skin Friction and Heat Transfer," presented at the Boundary Layer Research Meeting, London, England, 25-29 April 1960 under the sponsorship of the Wind Tunnel and Model Testing Panel, AGARD

(g) Klein, M., NBS, Private Communication, April 1960

(h) Hilsenrath, J. and Beckett, C., "Tables of Thermodynamic Properties of Argon-Free Air to 15,000°K," AEDC-TN-56-12, Arnold Engineering Development Center, September 1956

(i) Hilsenrath, J., et al., "Tables of Thermal Properties of Gases," National Bureau of Standards Circular 564, 1955

(j) Schmid, L., "Density Approximations for Argon-Free Air," NOL-TN-4718, 20 August 1959

(k) Dederick, L. S., "Construction and Selection of Smoothing Formulas," BRL Report 863, May 1953

(l) Hildenbrand, F. B., "Introduction to Numerical Analysis," McGraw-Hill Book Co., New York, 1956

TABLE I – A

COEFFICIENTS FOR FOURTH DEGREE VELOCITY
PROFILES FOR Λ^* LESS THAN 1.0

	a_0	a_1	a_2	a_3	a_4
H1(Λ^*)	0.	7.9365077E-02	0.	0.	-1.3468014E-03
H2(Λ^*)	0.	3.9682527E-03	0.	0.	-9.6200031E-05
H3(Λ^*)	0.	-5.2909901E-04	0.	0.	1.4028774E-05
H4(Λ^*)	0.	1.9841270E-02	-9.9206332E-03	0.	6.7340069E-04
H5(Λ^*)	0.	9.9206330E-04	-5.9523735E-04	0.	4.8099784E-05
H6(Λ^*)	0.	-1.3227455E-04	8.2671088E-05	0.	-7.0143577E-06
H7(Λ^*)	0.	3.3068787E-03	0.	-1.3888902E-03	4.4893333E-04
H8(Λ^*)	0.	1.6534392E-04	0.	-9.2592613E-05	3.2066688E-05
H9(Λ^*)	0.	-2.2045780E-05	0.	1.3227342E-05	-4.6762360E-06

	a_5	a_6
H1(Λ^*)	0.	0.
H2(Λ^*)	0.	0.
H3(Λ^*)	0.	0.
H4(Λ^*)	0.	0.
H5(Λ^*)	0.	0.
H6(Λ^*)	0.	0.
H7(Λ^*)	0.	0.
H8(Λ^*)	0.	0.
H9(Λ^*)	0.	0.

TABLE I – A

COEFFICIENTS FOR FOURTH DEGREE VELOCITY PROFILES FOR Δ* GREATER THAN 1.0

	a_0	a_{-1}	a_{-2}	a_{-3}	a_{-4}
$H_1(\Delta*)$	2.8571428E-01	-4.0000001E-01	2.2222224E-01	0.	0.
$H_2(\Delta*)$	9.5238090E-03	0.	-2.2222224E-02	2.3809526E-02	0.
$H_3(\Delta*)$	-1.1904743E-03	0.	1.8518520E-03	0.	-4.1666677E-03
$H_4(\Delta*)$	0.	3.3333332E-02	-2.7777775E-02	0.	0.
$H_5(\Delta*)$	0.	0.	2.7777773E-03	-3.5714284E-03	0.
$H_6(\Delta*)$	0.	0.	-2.3148145E-04	0.	6.9444436E-04
$H_7(\Delta*)$	0.	8.3333322E-03	-7.4074063E-03	0.	0.
$H_8(\Delta*)$	0.	0.	7.4074064E-04	-9.9206306E-04	0.
$H_9(\Delta*)$	0.	0.	-6.1728386E-05	0.	1.9841260E-04

	a_{-5}	a_{-6}	a_{-7}
$H_1(\Delta*)$	-7.4074103E-02	5.7142891E-02	-1.2987018E-02
$H_2(\Delta*)$	-1.4814818E-02	9.5238127E-03	-1.9480530E-03
$H_3(\Delta*)$	4.9382726E-03	-2.3809532E-03	4.3290061E-04
$H_4(\Delta*)$	1.3227511E-02	-1.0714280E-02	2.5252518E-03
$H_5(\Delta*)$	2.6455023E-03	-1.7857135E-03	3.7878774E-04
$H_6(\Delta*)$	-8.8183405E-04	4.4642836E-04	-8.4175043E-05
$H_7(\Delta*)$	3.8580224E-03	-3.1746011E-03	7.5757504E-04
$H_8(\Delta*)$	7.7160435E-04	-5.2910019E-04	1.1363628E-04
$H_9(\Delta*)$	-2.5720143E-04	1.3227505E-04	-2.5252506E-05

$$H_i(\Delta*) = \sum_i a_i(\Delta*)^i \text{ where } i = 0, 1, 2, \dots 6 \text{ for } \Delta* \text{ less than } 1.0$$

$$\text{and} \quad i = 0, -1, -2, \dots -7 \text{ for } \Delta* \text{ greater than } 1.0$$

2

TABLE I - B .

COEFFICIENTS FOR FIFTH DEGREE VELOCITY PROFILES FOR $\triangle*$ LESS THAN 1.0

	a_0	a_1	a_2	a_3	a_4	a_5	a_6
$H_1(\triangle*)$	0.	9.9206357E-02	0.	0.	-6.7340136E-03	2.1645073E-03	0.
$H_2(\triangle*)$	0.	4.9603152E-03	0.	0.	-4.8099831E-04	1.6233604E-04	0.
$H_3(\triangle*)$	0.	-6.6137266E-04	0.	0.	7.0144421E-05	-2.4048612E-05	0.
$H_4(\triangle*)$	0.	1.4880953E-02	-9.9205332E-03	0.	2.0202035E-03	-5.4112681E-04	0.
$H_5(\triangle*)$	0.	7.4404733E-04	-5.9523735E-04	0.	1.4430028E-04	-4.0584009E-05	0.
$H_6(\triangle*)$	0.	-9.9205934E-05	8.2671088E-05	0.	-2.1043175E-05	6.0121529E-06	0.
$H_7(\triangle*)$	0.	1.6534394E-03	0.	-1.3888902E-03	8.9786667E-04	-1.8037541E-04	0.
$H_8(\triangle*)$	0.	8.2671961E-05	0.	-9.2592613E-05	6.4133374E-05	-1.3528042E-05	0.
$H_9(\triangle*)$	0.	-1.1022890E-05	0.	1.3227342E-05	-9.3524721E-06	2.0040716E-06	0.

3

TABLE I - B

COEFFICIENTS FOR FIFTH DEGREE VELOCITY
PROFILES FOR Δ^* GREATER THAN 1.0

	a_0	a_{-1}	a_{-2}	a_{-3}	a_{-4}
$H_1(\Delta^*)$	2.8571428E-01	-3.3333333E-01	1.5873016E-01	0.	0.
$H_2(\Delta^*)$	9.5238090E-03	0.	-1.5873017E-02	1.4880951E-02	0.
$H_3(\Delta^*)$	-1.1904743E-03	0.	1.3227514E-03	0.	-2.3148147E-03
$H_4(\Delta^*)$	0.	1.6666667E-02	-1.1904761E-02	0.	0.
$H_5(\Delta^*)$	0.	0.	1.1904758E-03	-1.3392856E-03	0.
$H_6(\Delta^*)$	0.	0.	-9.9206334E-05	0.	2.3143162E-04
$H_7(\Delta^*)$	0.	2.7777764E-03	-2.1164007E-03	0.	0.
$H_8(\Delta^*)$	0.	0.	2.1164008E-04	-2.4801528E-04	0.
$H_9(\Delta^*)$	0.	0.	-1.7636672E-05	0.	4.4091539E-05

	a_{-5}	a_{-6}	a_{-7}
$H_1(\Delta^*)$	-3.7037045E-02	2.5974028E-02	-5.4112524E-03
$H_2(\Delta^*)$	-7.4074063E-03	4.3290034E-03	-8.1168765E-04
$H_3(\Delta^*)$	2.4691364E-03	-1.0822508E-03	1.8037506E-04
$H_4(\Delta^*)$	3.9682547E-03	-2.9220749E-03	6.3131329E-04
$H_5(\Delta^*)$	7.9365120E-04	-4.8701255E-04	9.4697111E-05
$H_6(\Delta^*)$	-2.6455056E-04	1.2175314E-04	-2.1043786E-05
$H_7(\Delta^*)$	7.7160214E-04	-5.7719787E-04	1.2626161E-04
$H_8(\Delta^*)$	1.5432027E-04	-9.6199683E-05	1.8939259E-05
$H_9(\Delta^*)$	-5.1440029E-05	2.4049921E-05	-4.2087231E-06

$H_i(\Lambda^*) = \sum_i a_i(\Delta^*)^i$ where $i = 0, 1, 2, \ldots 6$ for Λ^* less than 1.0

and $i = 0, -1, -2, \ldots -7$ for Λ^* greater than 1.0

TABLE I -- C

COEFFICIENTS FOR SIXTH DEGREE VELOCITY
PROFILES FOR Λ^* LESS THAN 1.0

	a_0	a_1	a_2	a_3	a_4	a_5	a_6
$H_1(\Lambda^*)$	0.	1.1904763E-01	0.	0.	-2.0202011E-02	1.2987047E-02	-2.4975017E-03
$H_2(\Lambda^*)$	0.	5.9523786E-03	0.	0.	-1.4429949E-03	9.7402184E-04	-1.9424921E-04
$H_3(\Lambda^*)$	0.	-7.9364749E-04	0.	0.	2.1043117E-04	-1.4429353E-04	2.9136310E-05
$H_4(\Lambda^*)$	0.	1.1904764E-02	-9.9206332E-03	0.	4.0404039E-03	-2.1645073E-03	3.7462451E-04
$H_5(\Lambda^*)$	0.	5.9523810E-04	-5.9523735E-04	0.	2.8860057E-04	-1.6233604E-04	2.9137358E-05
$H_6(\Lambda^*)$	0.	-7.9364749E-05	8.2671088E-05	0.	-4.2086350E-05	2.4048612E-05	-4.3703620E-06
$H_7(\Lambda^*)$	0.	9.9206361E-04	0.	-1.3888902E-03	1.3468014E-03	-5.4112681E-04	8.3249991E-05
$H_8(\Lambda^*)$	0.	4.9603148E-05	0.	-9.2592613E-05	9.6200031E-05	-4.0584009E-05	6.4749765E-06
$H_9(\Lambda^*)$	0.	-6.6137254E-06	0.	1.3227342E-05	-1.4028774E-05	6.0121529E-06	-9.7117660E-07

TABLE I - C

COEFFICIENTS FOR SIXTH DEGREE VELOCITY
PROFILES FOR Λ^* GREATER THAN 1.0

	a_0	a_{-1}	a_{-2}	a_{-3}	a_{-4}
$H_1(\Lambda^*)$	2.3571428E-01	-2.3571428E-01	1.1904763E-01	0.	0.
$H_2(\Lambda^*)$	9.5233090E-03	0.	-1.1904764E-02	9.9206305E-03	0.
$H_3(\Lambda^*)$	-1.1904743E-03	0.	9.9206361E-04	0.	-1.3888897E-03
$H_4(\Lambda^*)$	0.	9.5238090E-03	-5.9523806E-03	0.	0.
$H_5(\Lambda^*)$	0.	0.	5.9523787E-04	-5.9523735E-04	9.2592787E-05
$H_6(\Lambda^*)$	0.	0.	-4.9603148E-05	0.	0.
$H_7(\Lambda^*)$	0.	1.1904743E-03	-7.9364842E-04	0.	0.
$H_8(\Lambda^*)$	0.	0.	7.9364864E-05	-3.2671204E-05	0.
$H_9(\Lambda^*)$	0.	0.	-6.6137400E-06	0.	1.3227371E-05

	a_{-5}	a_{-6}	a_{-7}
$H_1(\Lambda^*)$	-2.0202041E-02	1.2987070E-02	-2.4974942E-03
$H_2(\Lambda^*)$	-4.0404069E-03	2.1645091E-03	-3.7462218E-04
$H_3(\Lambda^*)$	1.3468042E-03	-5.4712728E-04	8.3249643E-05
$H_4(\Lambda^*)$	1.4430024E-03	-9.7401997E-04	1.9424967E-04
$H_5(\Lambda^*)$	2.8360057E-04	-1.6233721E-04	2.9137591E-05
$H_6(\Lambda^*)$	-9.6200731E-05	4.0584301E-05	-6.4750347E-06
$H_7(\Lambda^*)$	2.1043187E-04	-1.4429493E-04	2.9136427E-06
$H_8(\Lambda^*)$	4.2086350E-05	-2.4049135E-05	4.3704785E-06
$H_9(\Lambda^*)$	-1.4028861E-05	6.0122837E-06	-9.7122027E-07

$H_i(\Lambda^*) = \sum_i a_i(\Lambda^*)^i$ where $i = 0, 1, 2, \ldots 6$ for Λ^* less than 1.0

and $= 0, -1, -2, \ldots -7$ for Λ^* greater than 1.0

TABLE I - D

NUMERICAL VALUES OF α_i

Alphas for Fourth Degree Velocity Profiles

α_0	α_1	α_2	α_3	α_4	α_5
5.9999993E-01	3.3333332E-02	8.3333322E-03	4.5679010E-01	1.4991169E-03	9.3082503E-05

α_6	α_7	α_8
1.7636682E-02	4.6310691E-03	3.7110522E-04

Alphas for Fifth Degree Velocity Profiles

α_0	α_1	α_2	α_3	α_4	α_5
6.6666666E-01	1.6666667E-02	2.7777764E-03	5.4240820E-01	4.2339198E-04	1.1579606E-05

α_6	α_7	α_8
9.0848953E-03	1.6026665E-03	6.9644796E-05

Alphas for Sixth Degree Velocity Profiles

α_0	α_1	α_2	α_3	α_4	α_5
7.1428571E-01	9.5238090E-03	1.1904743E-03	6.0495055E-01	1.5540142E-04	2.3740977E-06

α_6	α_7	α_8
5.2891546E-03	6.9837399E-04	1.9101790E-05
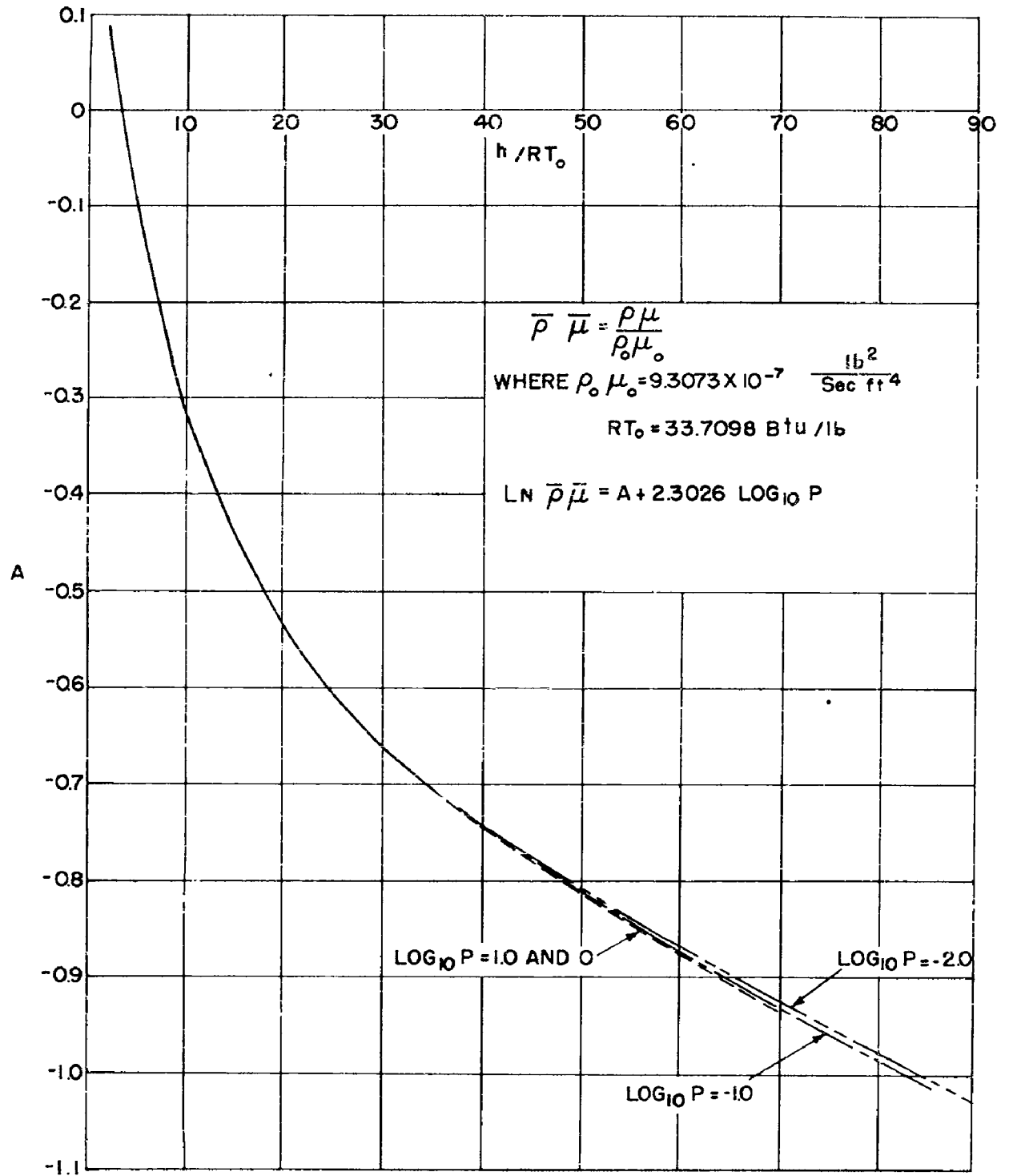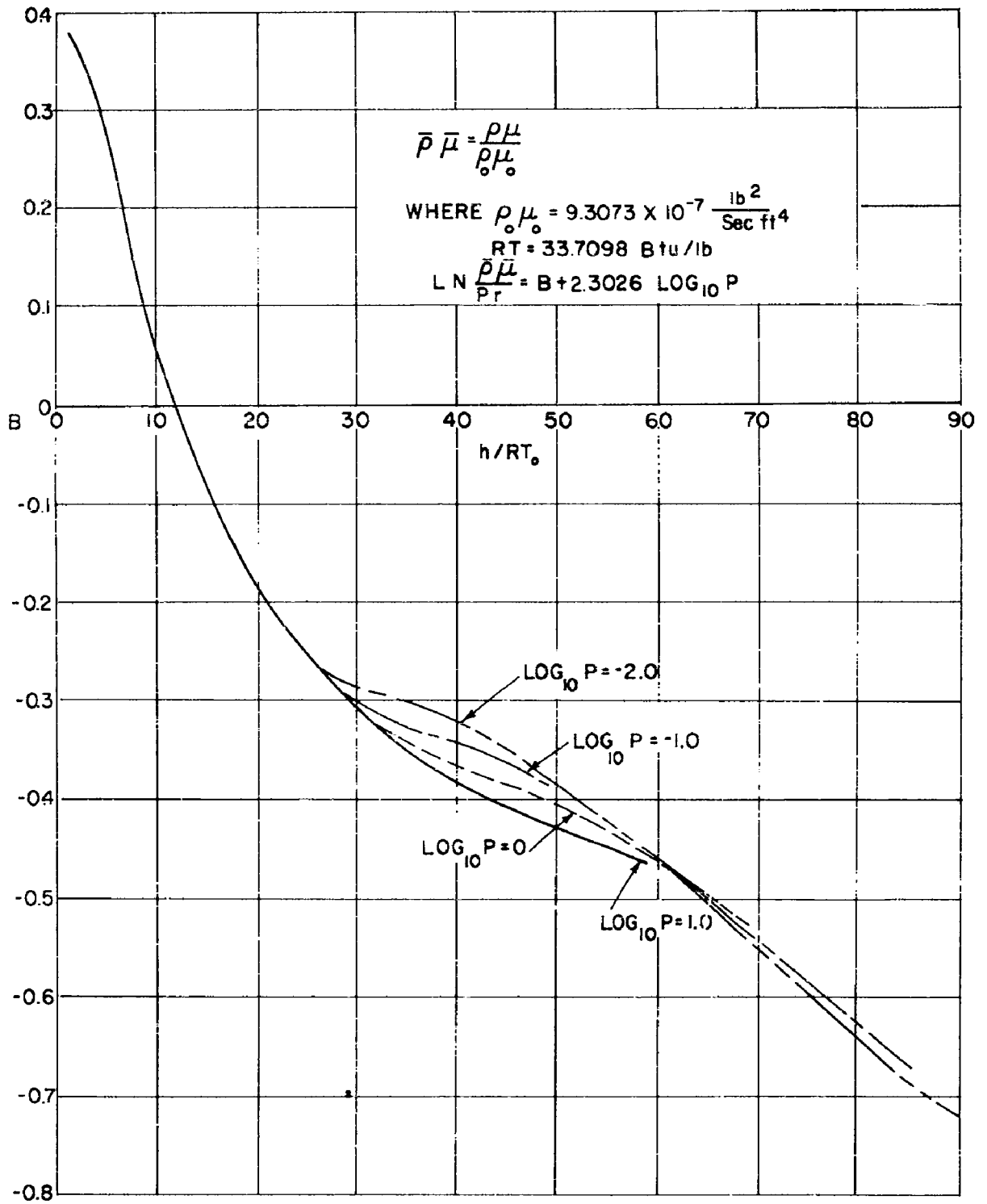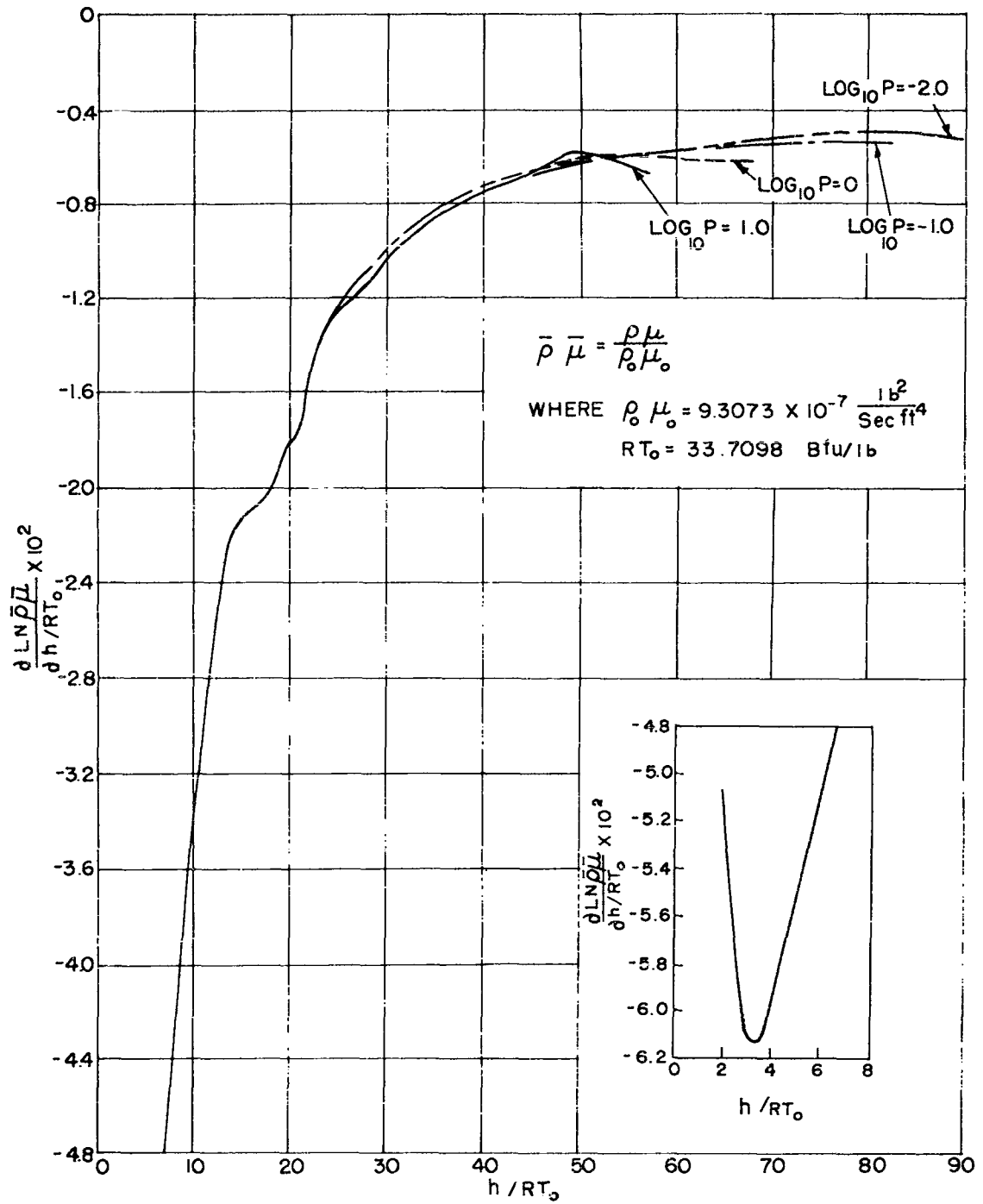
$$\overline{\rho}\,\overline{\mu} = \frac{\rho\mu}{\rho_o\mu_o}$$

WHERE $\rho_o\,\mu_o = 9.3073 \times 10^{-7} \quad \frac{lb^2}{Sec\ ft^4}$

$RT_o = 33.7098\ Btu/lb$

$LN\ \overline{\rho}\overline{\mu} = A + 2.3026\ LOG_{10}\ P$

$LOG_{10}\ P = 1.0\ AND\ 0$

$LOG_{10}\ P = -2.0$

$LOG_{10}\ P = -1.0$

FIG. 1-A $LN\ \overline{\rho}\,\overline{\mu}$ VS h/RT_o

$$\bar{\rho}\,\bar{\mu} = \frac{\rho\mu}{\rho_o\mu_o}$$

WHERE $\rho_o\mu_o = 9.3073 \times 10^{-7} \frac{lb^2}{Sec\,ft^4}$

$RT = 33.7098\ Btu/lb$

$LN \frac{\bar{\rho}\bar{\mu}}{Pr} = B + 2.3026\ LOG_{10}\ P$

$LOG_{10} P = -2.0$

$LOG_{10} P = -1.0$

$LOG_{10} P = 0$

$LOG_{10} P = 1.0$

FIG. I-B $LN \frac{\bar{\rho}\bar{\mu}}{Pr}$ VS h/RT_o

FIG. I-C $\frac{\partial LN \bar{\rho}\bar{\mu}}{\partial h/RT_o}$ VS h/RT$_o$

FIG. I-D $\dfrac{\partial LN \dfrac{(\overline{\rho}\overline{\mu})}{Pr}}{\partial \left(\dfrac{h}{RT_o}\right)}$ VS $^h/RT_o$

$$\bar{\rho}\,\bar{\mu} = \frac{\rho\,\mu}{\rho_o\,\mu_o}$$

WHERE $\rho_o\,\mu_o = 9.3073 \times 10^{-7}\,\dfrac{lb^2}{Sec\,ft^4}$

$R\,T_o = 33.7098$ Btu/lb

FIG. I-E $\dfrac{\partial^2 LN\,\bar{\rho}\,\bar{\mu}}{\partial\,(h/RT_o)^2}$ VS h/RT_o

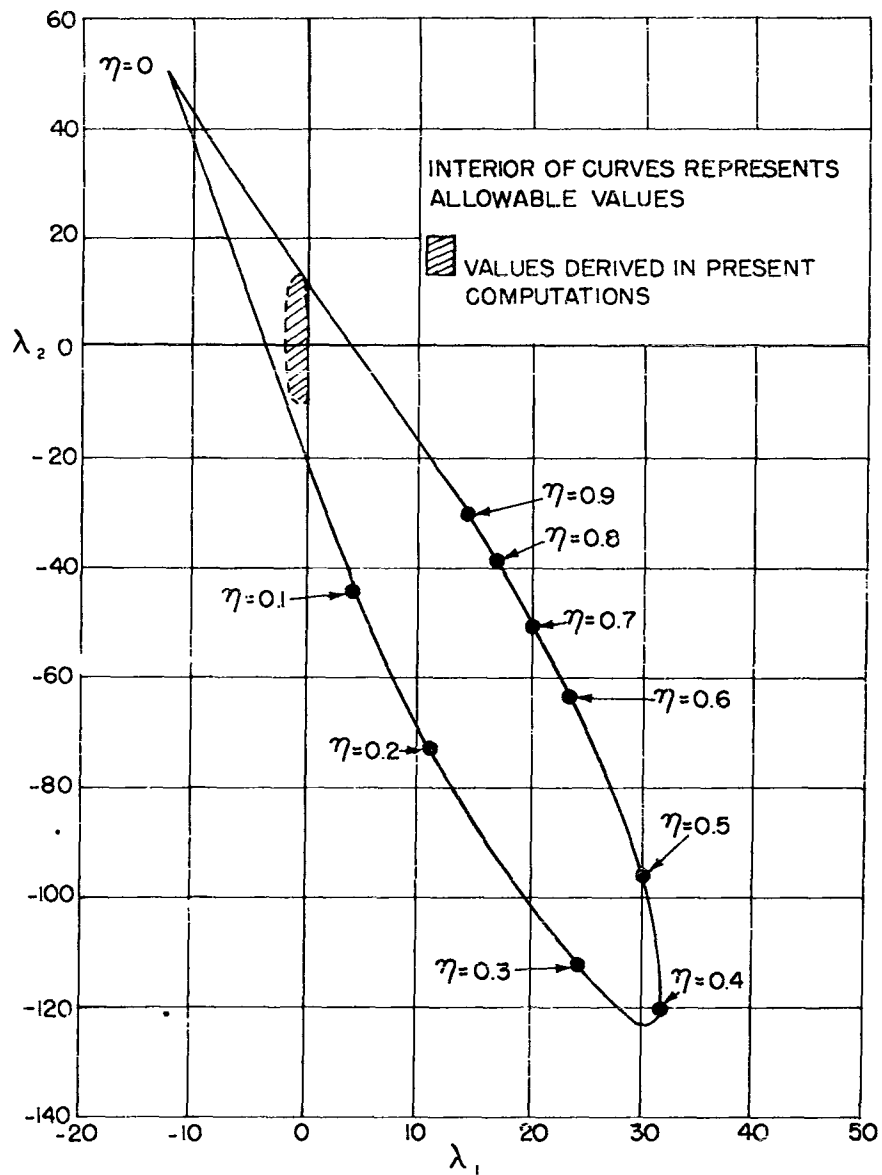FIG. 1-F $\dfrac{\partial^2 LN (\bar{\rho}\bar{\mu}/Pr)}{\partial (h/RT_o)^2}$ VS h/RT_o
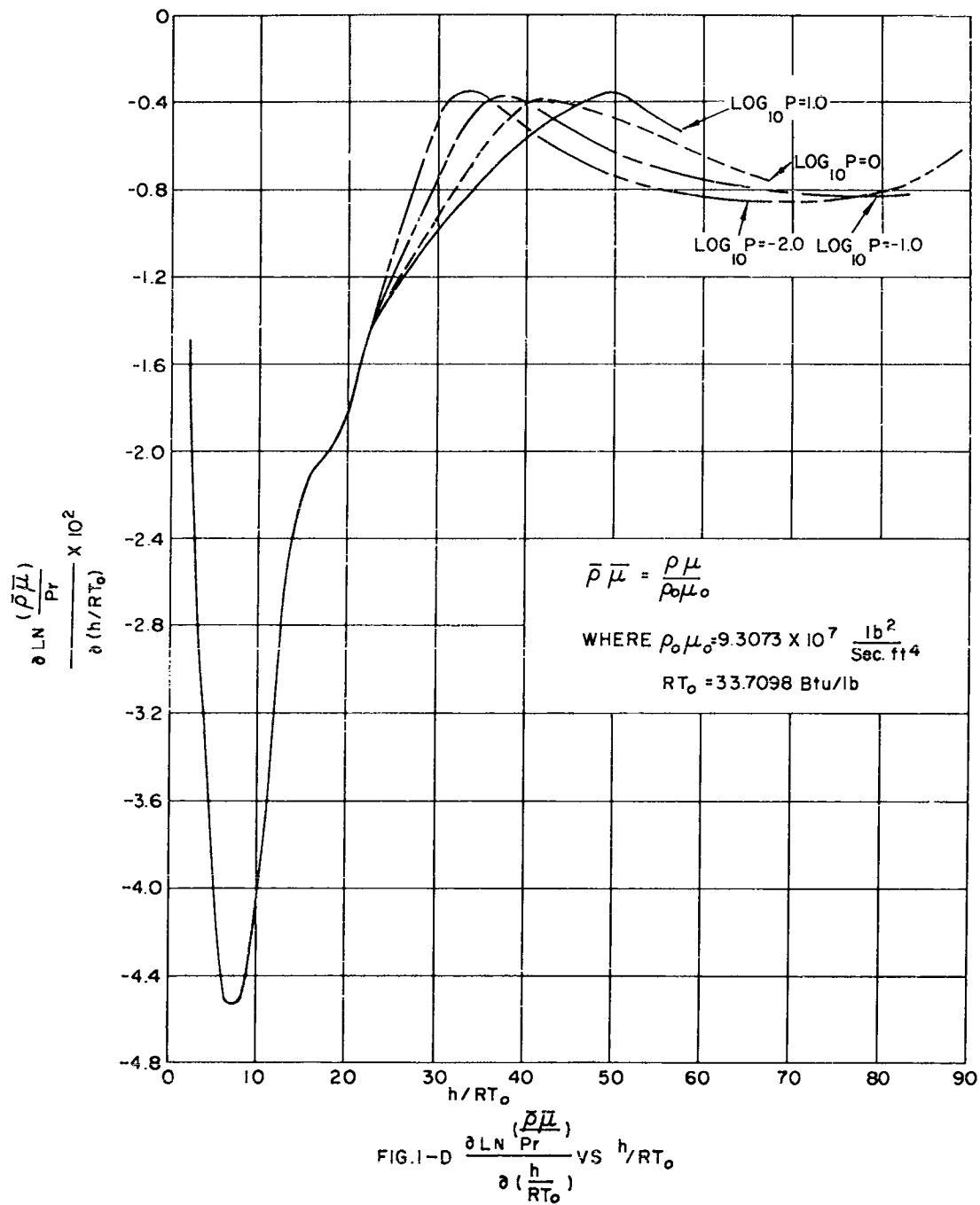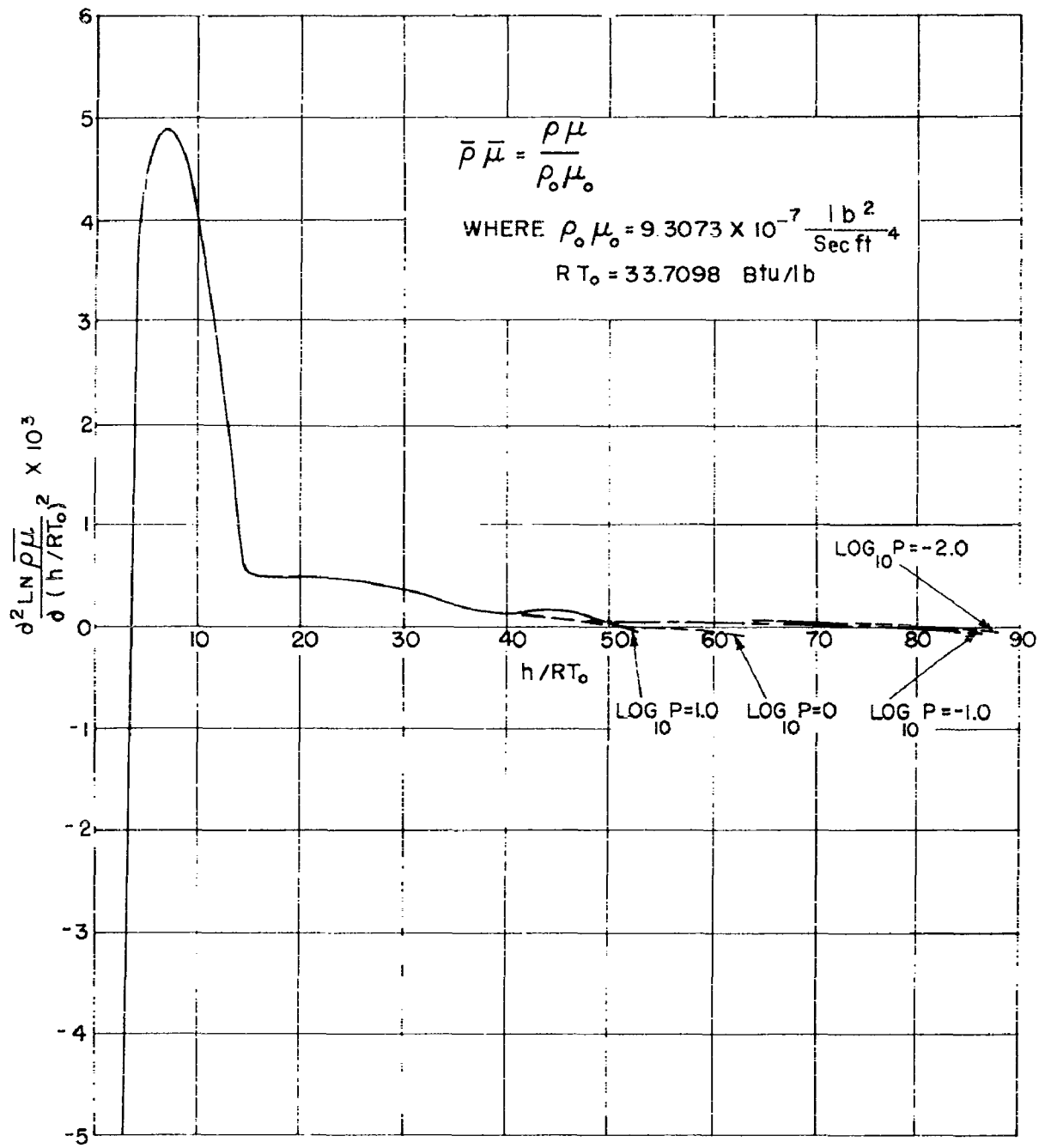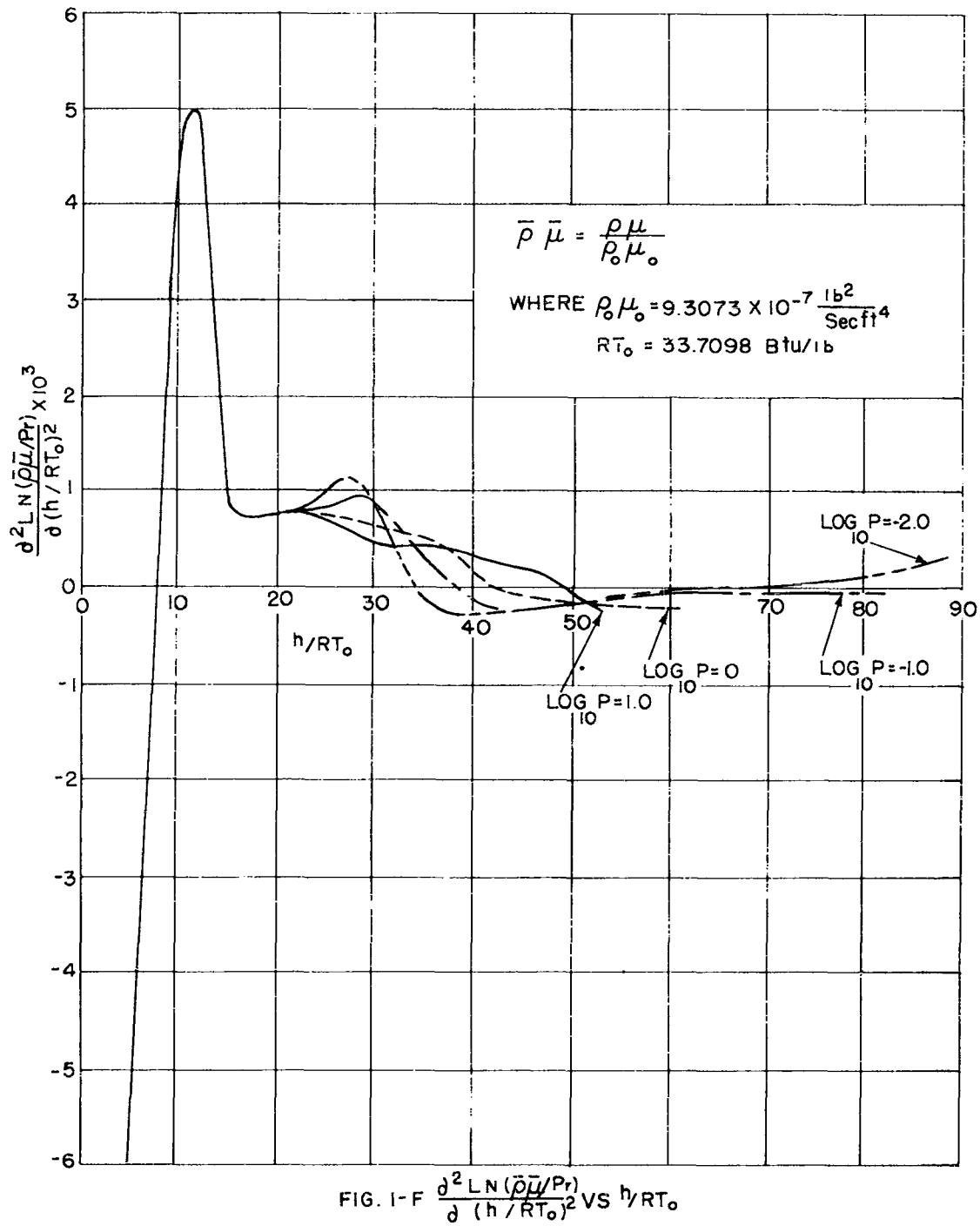
FIG. 2-A VELOCITY PROFILE PARAMETER LIMITATIONS,
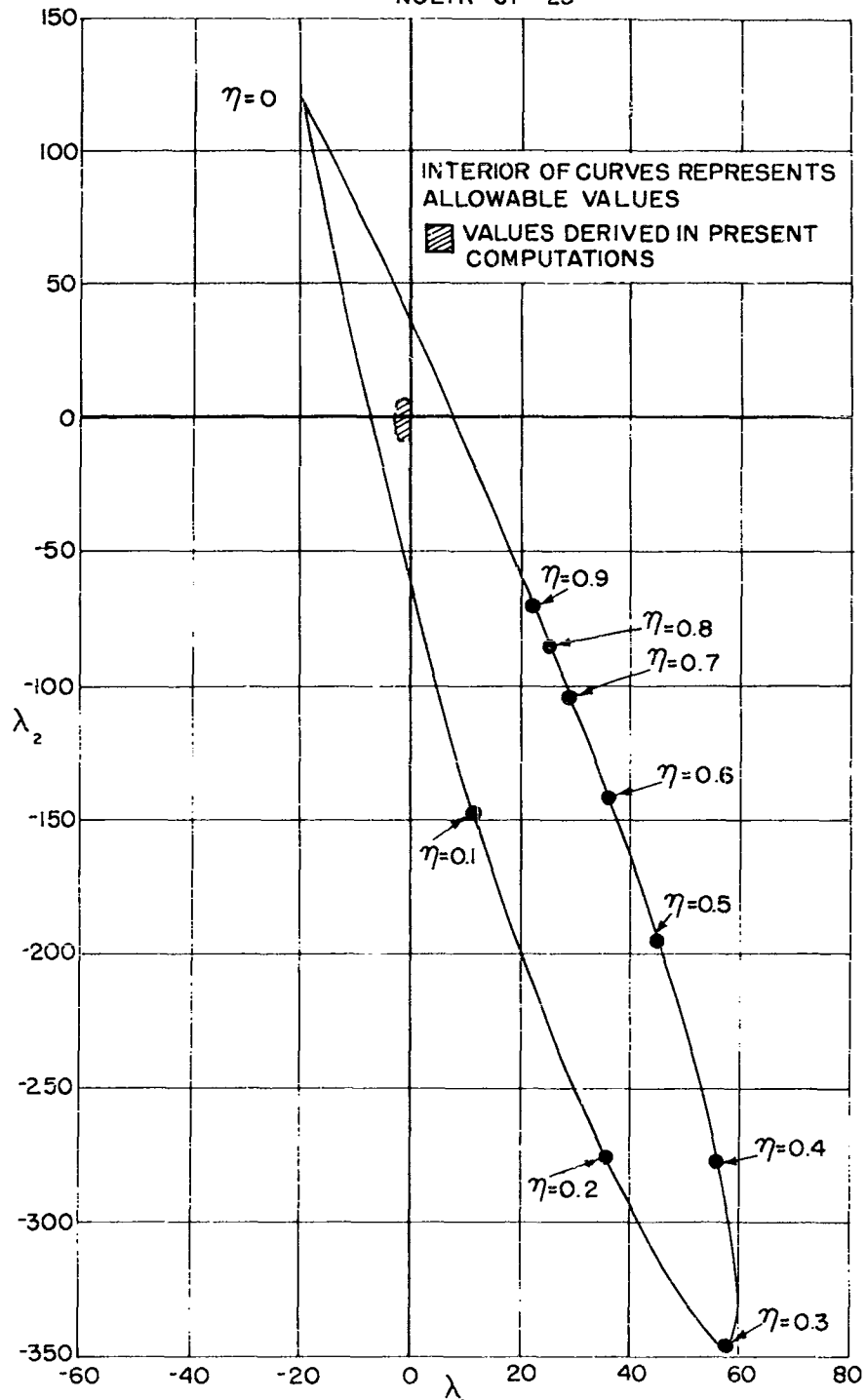FOURTH DEGREE POLYNOMIALS

FIG. 2-B VELOCITY PROFILE PARAMETER LIMITATIONS,
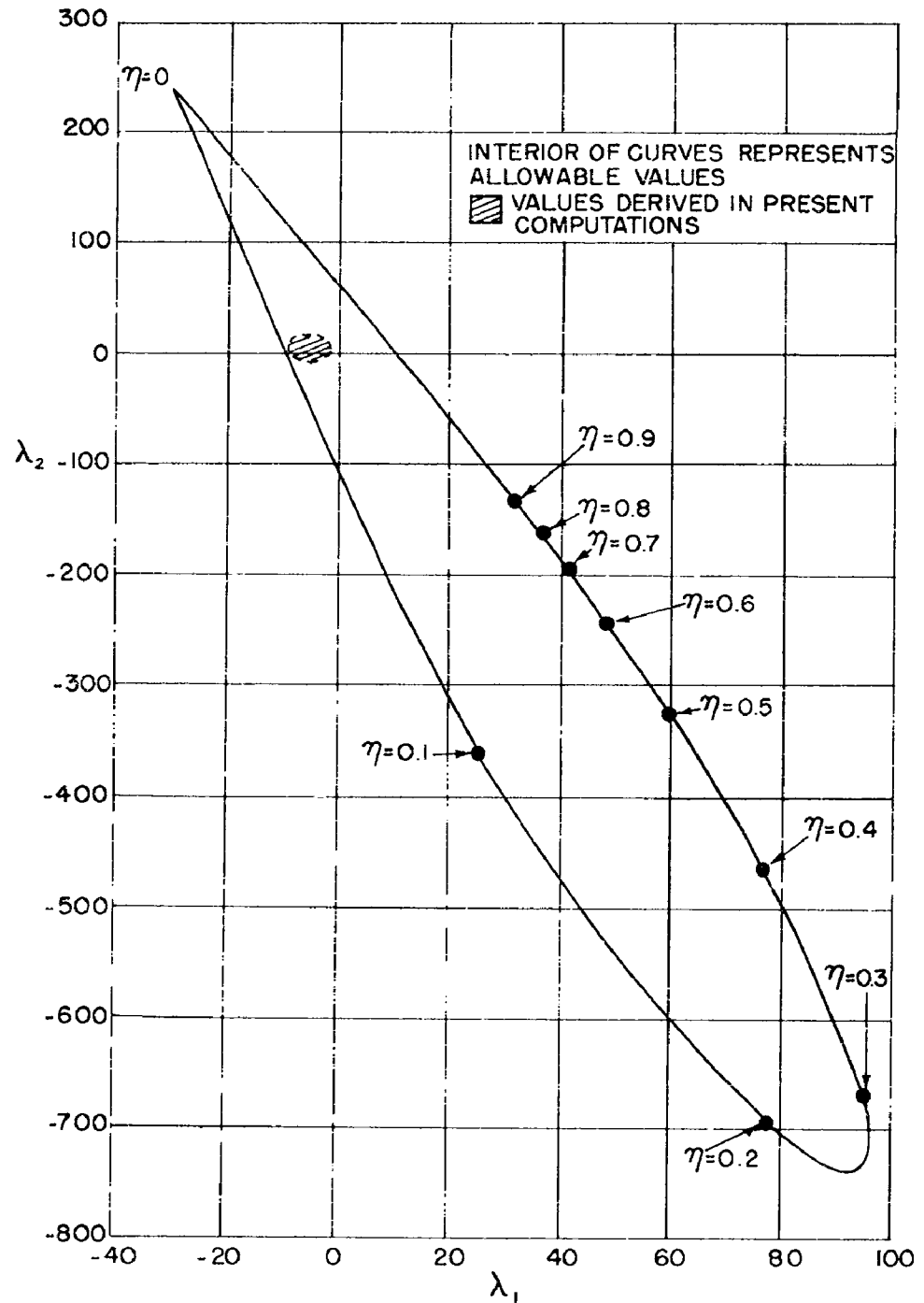FIFTH DEGREE POLYNOMIALS

FIG. 2C VELOCITY PROFILE PARAMETER LIMITATIONS,
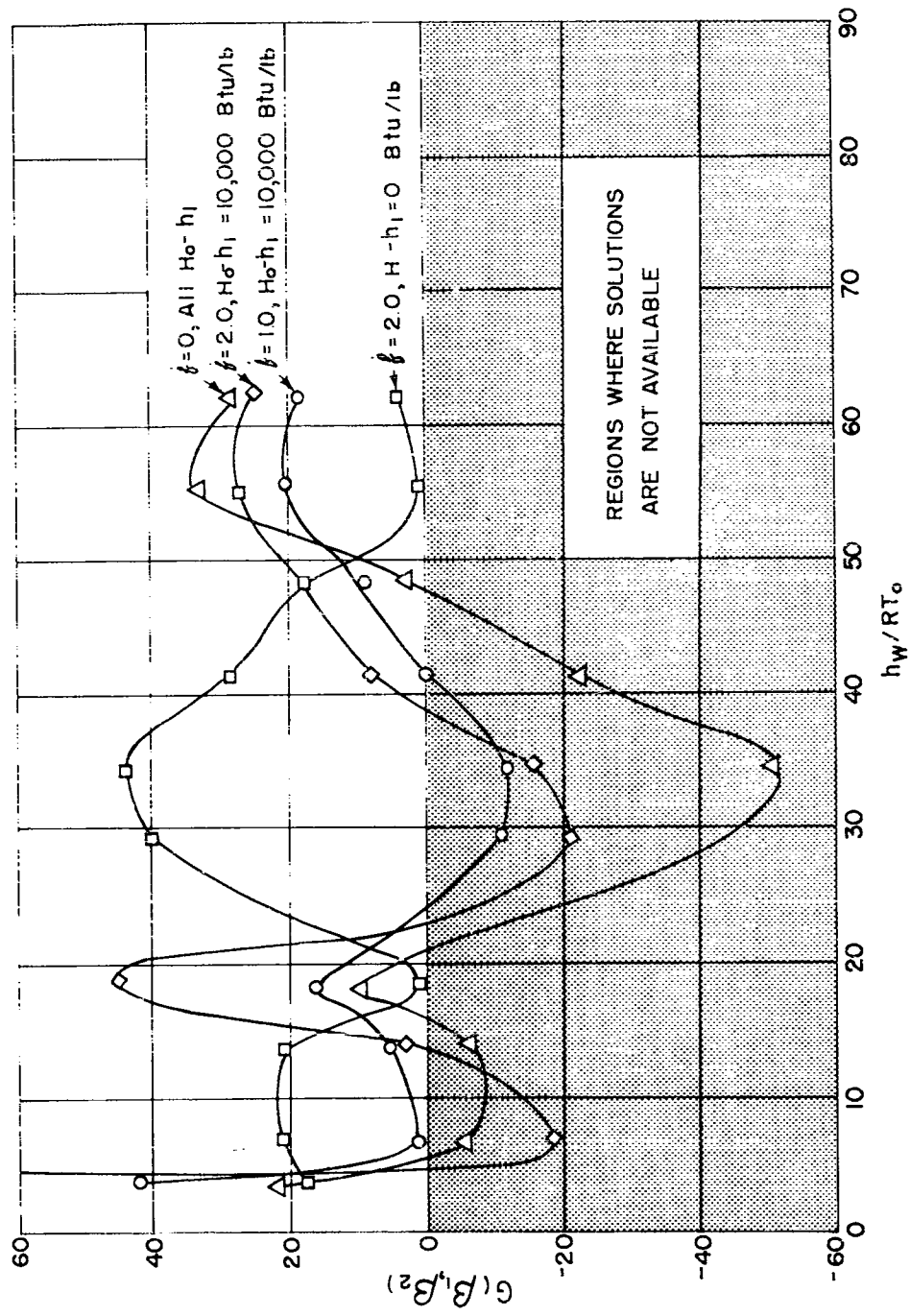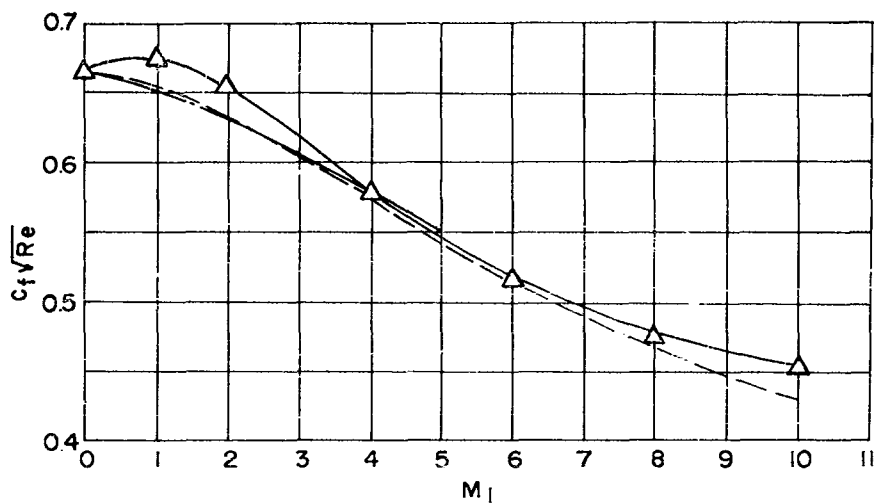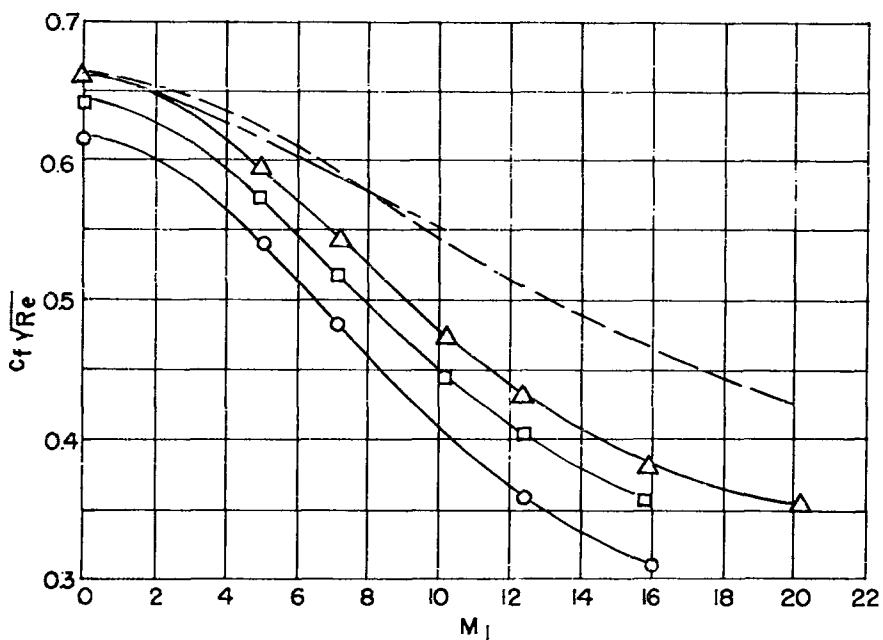SIXTH DEGREE POLYNOMIALS

FIG. 3 PROPERTY VALUE CRITERION

(a) ZERO HEAT TRANSFER, STATIC ENTHALPY

(b) $T_W / T_I = 1.0$ TOTAL ENTHALPY PROFILES USED
   $P = 1.0$ ATMOSPHERE

O 4TH DEGREE POLYNOMIALS
□ 5TH DEGREE POLYNOMIALS   — — — REFERENCE (c)
△ 6TH DEGREE POLYNOMIALS   —·— REFERENCE (e)

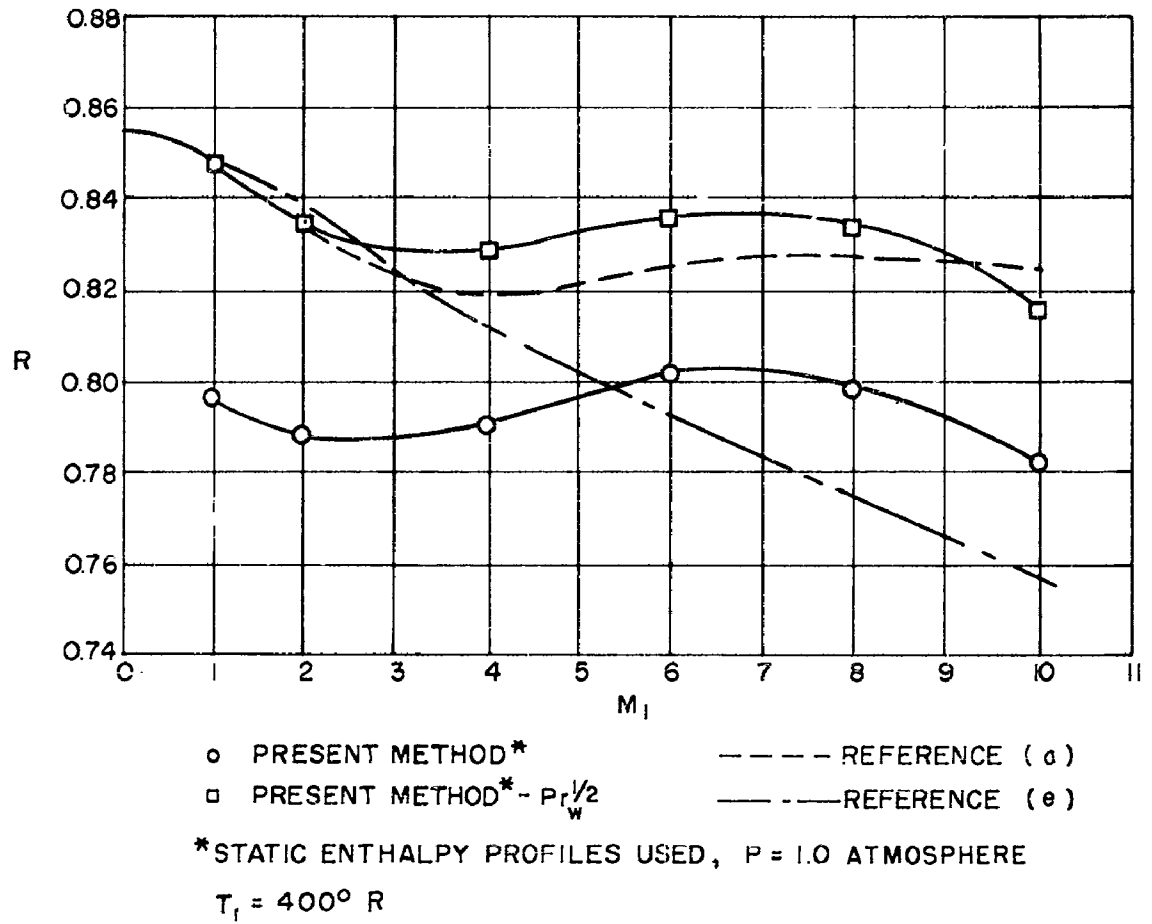FIG. 4 $C_f \sqrt{Re}$ VS M_I

FIG. 5 ENTHALPY RECOVERY FACTOR
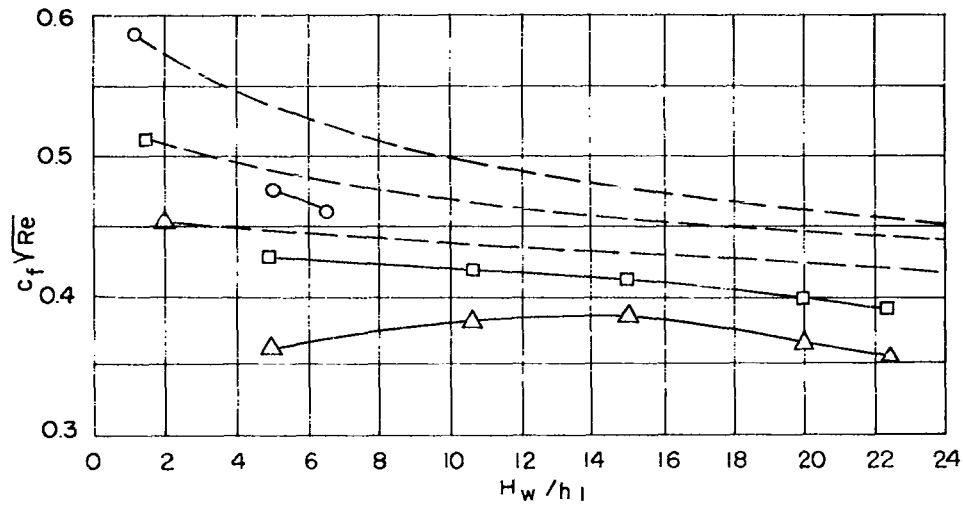
(a) 4TH DEGREE POLYNOMIAL VELOCITY PROFILES,
P = 0.1 ATMOSPHERES h_1 = 93.24 Btu/lb
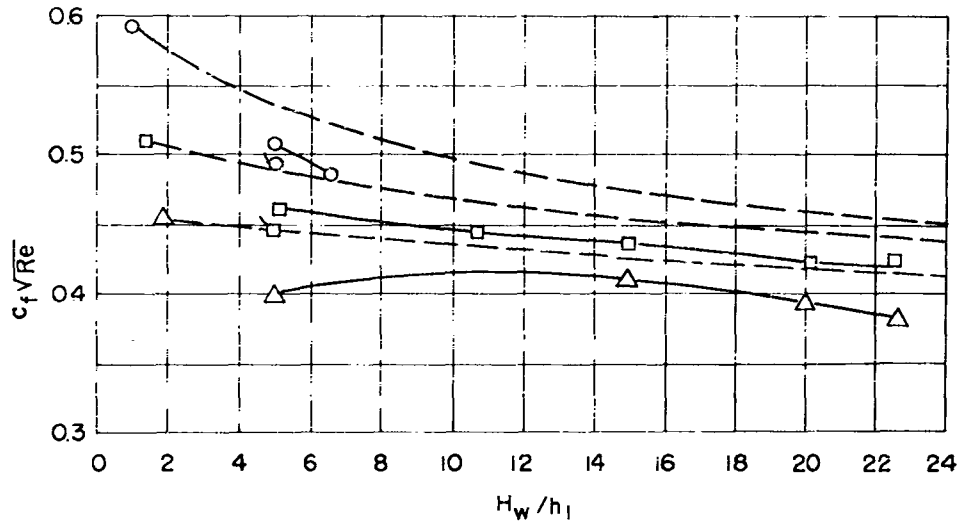
(b) 6TH DEGREE POLYNOMIAL VELOCITY PROFILES,
(TAGGED SYMBOLS FOR 5TH DEGREE POLYNOMIALS)
P = 0.1 ATMOSPHERES h_1 = 93.24 Btu/lb

○ $U^2/2h_1$ = 10   — — REFERENCE (f)
□ $U^2/2h_1$ = 30
△ $U^2/2h_1$ = 80

FIG. 6 $c_f \sqrt{Re}$ VS H_w/h_1

(a) 4TH DEGREE POLYNOMIAL VELOCITY PROFILES,
P = 0.1 ATMOSPHERES h_1 = 466.2 Btu/lb

(b) 6TH DEGREE POLYNOMIAL VELOCITY PROFILES
P = 0.1 ATMOSPHERES h_1 = 466.2 Btu/lb

O $U^2/2h_1$ = 10   — — — REFERENCE (f)
□ $U^2/2h_1$ = 30

FIG. 7 $c_f\sqrt{Re}$ VS H_w/h_1

(a) $h_I = 93.24$ Btu/lb   P = 0.1 ATMOSPHERES

(b) $h_I = 466.2$ Btu/lb
○ $U^2/2h_I = 10$
□ $U^2/2h_I = 30$
△ $U^2/2h_I = 80$
--- REFERENCE (f)

P = 0.1 ATMOSPHERES
OPEN SYMBOLS FOR THE 4TH DEGREE
POLYNOMIAL VELOCITY PROFILES AND
SHADED SYMBOLS FOR 6TH DEGREE
POLYNOMIALS

FIG. 8 MODIFIED REYNOLDS ANALOGY PARAMETER

O $U^2/2h_1 = 10$
□ $U^2/2h_1 = 30$
△ $U^2/2h_1 = 80$

— — — REFERENCE (f)

OPEN SYMBOLS FOR 4TH DEGREE
POLYNOMIAL VELOCITY PROFILES
AND SHADED SYMBOLS FOR 6TH
DEGREE POLYNOMIALS
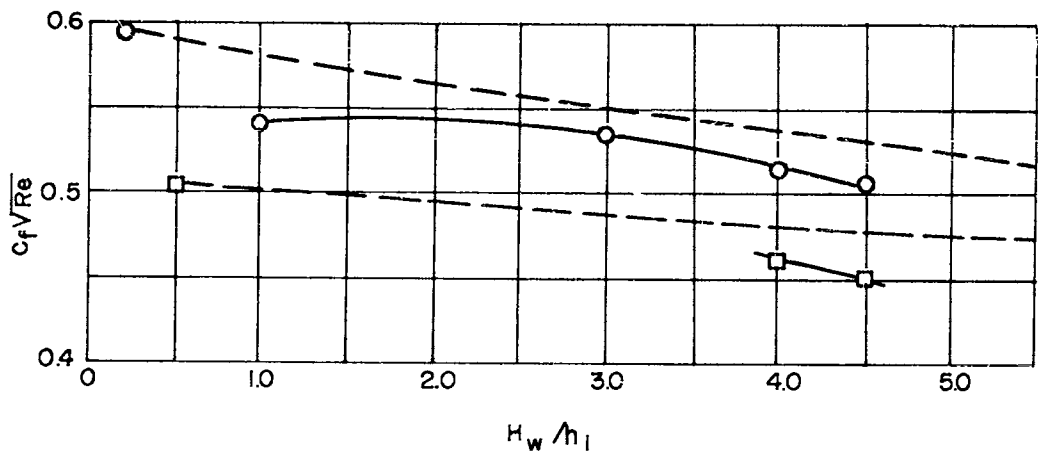
P = 0.1 ATMOSPHERES
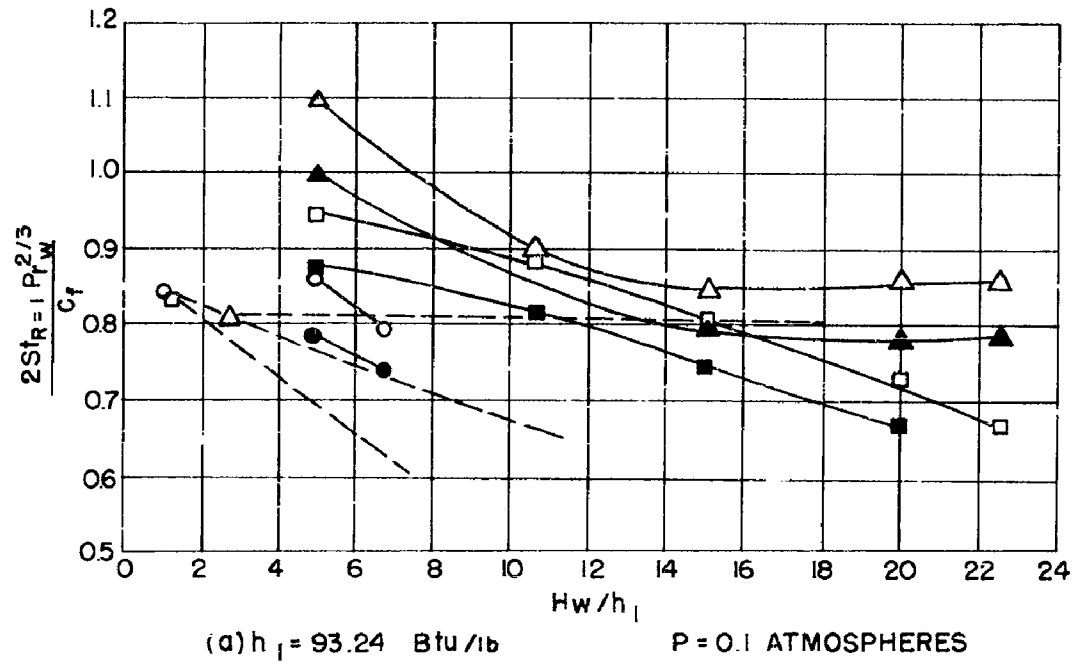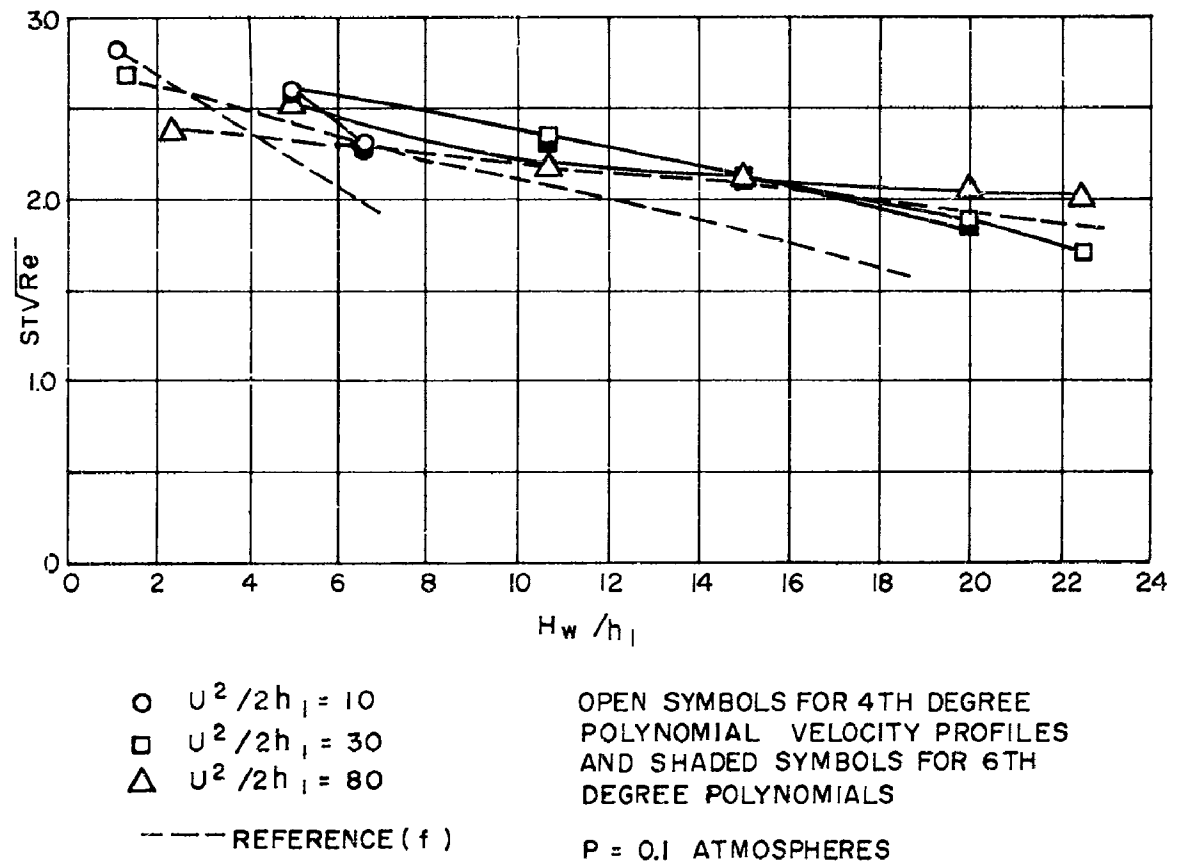
FIG. 9 $ST\sqrt{Re}$ VS H_w/h_1
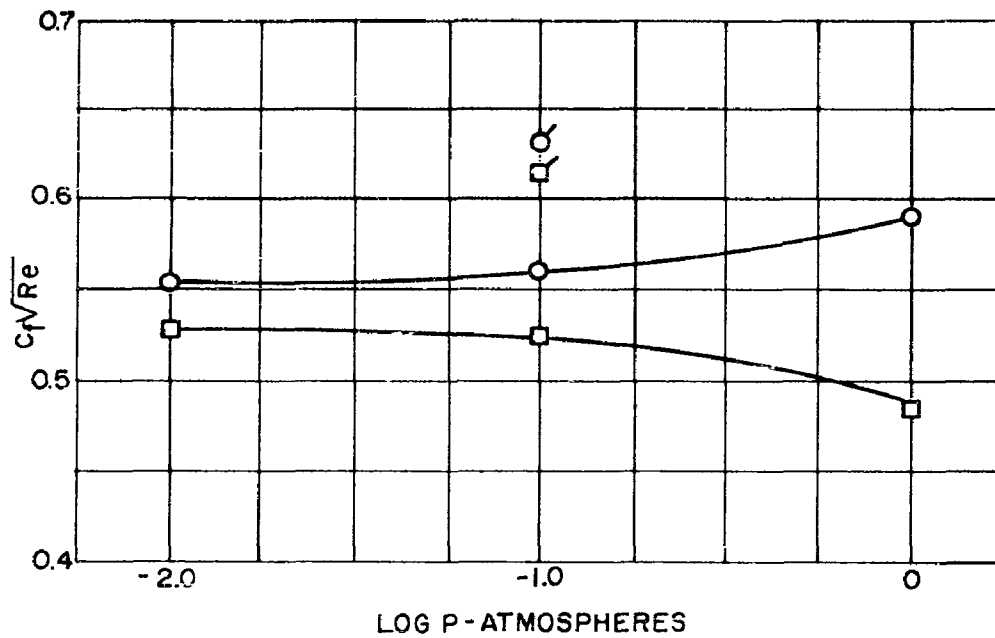
(a) 4TH DEGREE POLYNOMIAL VELOCITY PROFILES
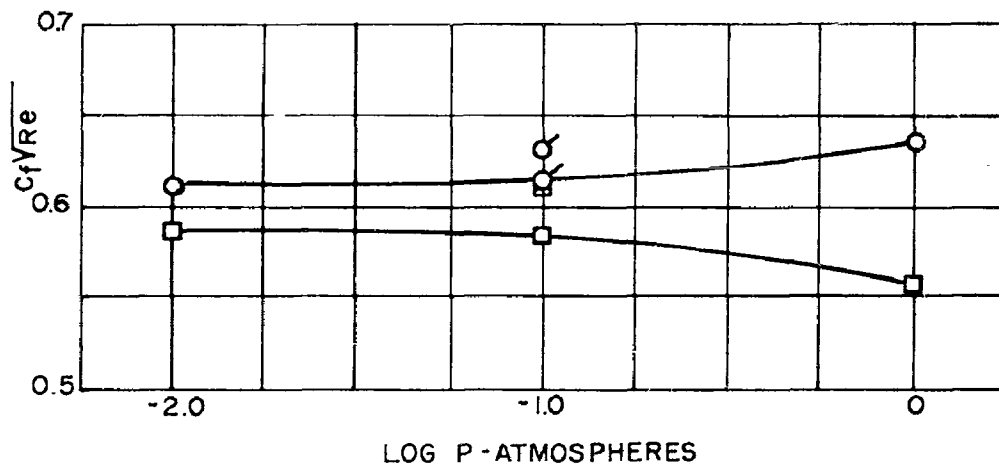
(b) 6TH DEGREE POLYNOMIAL VELOCITY PROFILES

O $H_w/h_1 = 0.7$ $h_1 = 2331$ Btu/lb

□ $H_w/h_1 = 0.9$ $U^2/2h_1 = 5.0$

TAGGED SYMBOLS REFERENCE (f) BY INTERPOLATION

FIG. 10 $C_f\sqrt{Re}$ VS PRESSURE LEVEL
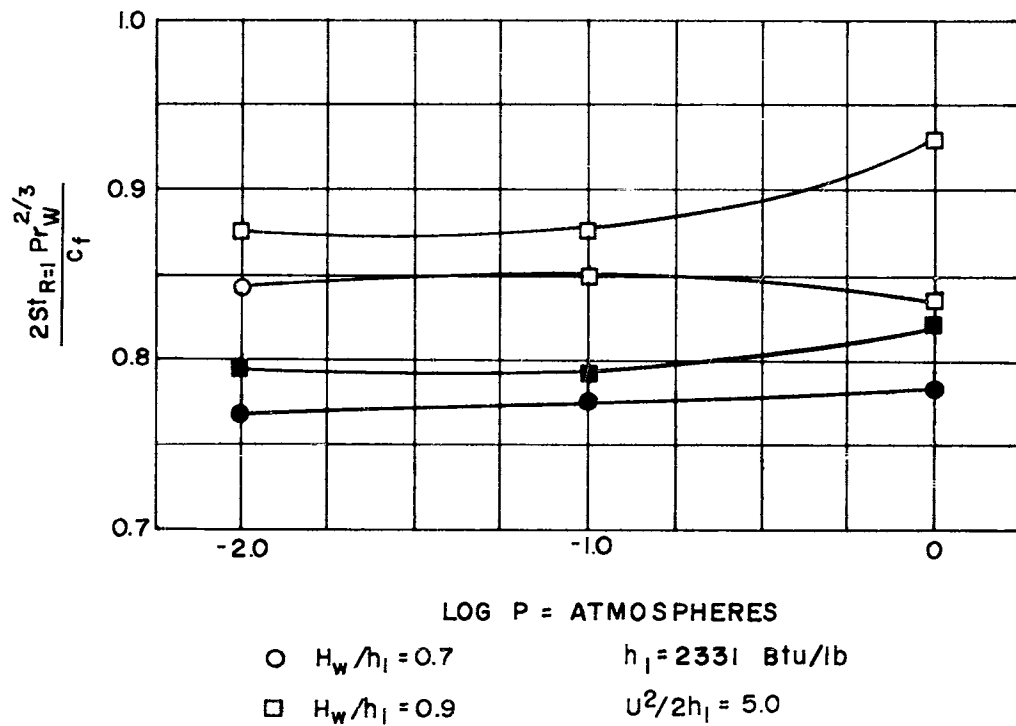
LOG P = ATMOSPHERES

O H_w/h_I = 0.7 h_I = 2331 Btu/lb

□ H_w/h_I = 0.9 $u^2/2h_I$ = 5.0

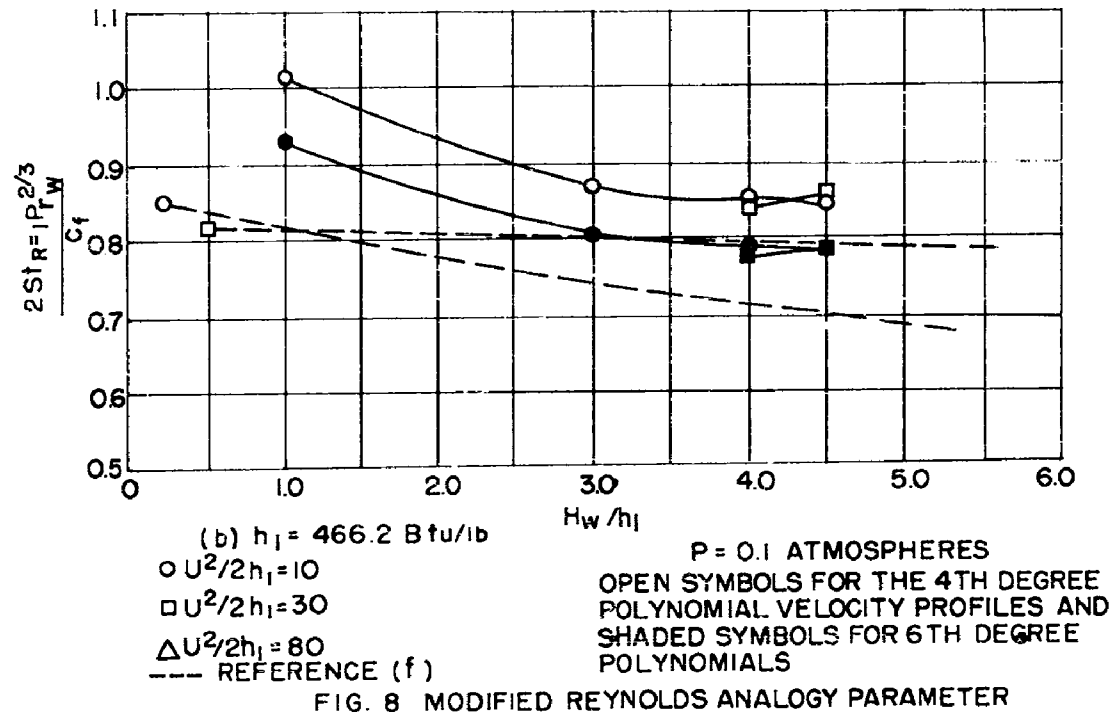OPEN SYMBOLS FOR 4TH DEGREE POLYNOMIAL VELOCITY
PROFILES AND SHADED SYMBOLS FOR 6TH DEGREE POLYNOMIALS

FIG. II MODIFIED REYNOLDS ANALOGY PARAMETER VS PRESSURE LEVEL

(a) VELOCITY PROFILE

(b) STATIC ENTHALPY PROFILE

P = 0.1 ATMOSPHERES
$U_1 = 11975$ ft/Sec
$H_w = h_1 = 95.5$ Btu/lb

o PRESENT METHOD 6TH DEGREE
POLYNOMIAL VELOCITY PROFILE
△ REFERENCE (f)

FIG. 12 NON-DIMENSIONAL PROFILES
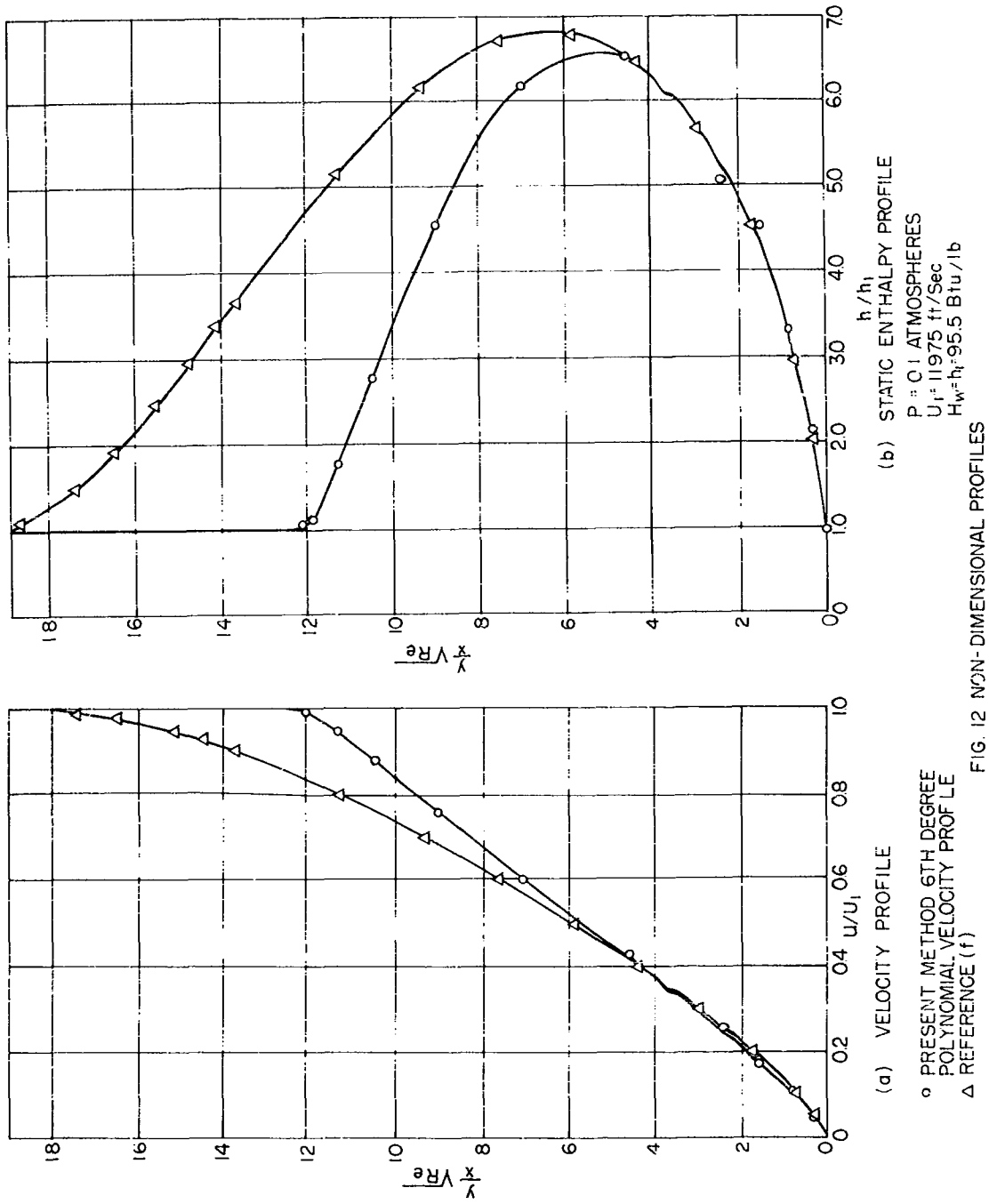
AERODYNAMICS DEPARTMENT
EXTERNAL DISTRIBUTION LIST (SP)

No. of Copies		No. of Copies	
	Chief, Bureau of Naval Weapons Department of the Navy Washington 25, D. C.		NASA Langley Research Center Langley Field, Virginia
1	Attn: RMMO	1	Attn: Librarian
1	Attn: RMGA	1	Attn: C. H. McLellan
1	Attn: RRMA	1	Attn: J. J. Stack
		1	Attn: Adolf Busemann
	Director, Special Projects Department of the Navy Washington 25, D. C.	1	Attn: R. W. Peters Structures Res. Div.
4	Attn: SP-20	1	Attn: R. Hopko, PARD
2	Attn: SP-27		
1	Attn: SP-272		NASA Ames Research Center Moffett Field, California
	Office of Naval Research Room 2709 - T-3 Washington 25, D. C.	1	Attn: Librarian
1	Attn: Head, Mechanics Br.		NASA Lewis Research Center 21000 Brookpark Road Cleveland, Ohio
5	Commanding Officer Office of Naval Research Branch Office, Box 39, Navy 100 Fleet Post Office New York, N. Y.	1	Attn: Chief, Propulsion Aerodynamics Div.
		2	Attn: Mr. G. Mandel, Chief, Library
	Director, DTMB Aerodynamics Laboratory Washington 7, D. C.		Office of the Assistant Secretary of Defense (R&D) Room 3E1041, The Pentagon Washington 25, D. C.
1	Attn: Library	1	Attn: Library (Technical)
	Naval Weapons Laboratory Dahlgren, Virginia		Research and Development Bd. Room 3D1041, The Pentagon Washington 25, D. C.
1	Attn: Library	1	Attn: Library
	Commander U. S. Naval Ordnance Test Station China Lake, California		ASTIA Arlington Hall Station Arlington 12, Virginia
1	Attn: Technical Library	10	Attn: TIPDR
	Director Naval Research Laboratory Washington 25, D. C.		Commander, NMC Point Mugu, California
1	Attn: Code 2027	1	Attn: Technical Library
1	Attn: Mr. E. Chapin Code 6310		

AERODYNAMICS DEPARTMENT
EXTERNAL DISTRIBUTION LIST (SP)

No. of
Copies

		No. of Copies	

Commanding General
Aberdeen Proving Ground, Md.
1   Attn: Technical Info. Br.
1   Attn: Ballistic Res. Lab.

Director of Intelligence
Headquarters, USAF
Washington 25, D. C.
1   Attn: AFOIN-3B

Commander
Wright Air Development Div.
Wright-Patterson AFB, Ohio
2   Attn: WCOSI-3
1   Attn: WCLSW-5
3   Attn: WCRRD

Commander, AFBMD
Air Res. & Develop. Command
P. O. Box 262
Inglewood, California
1   Attn: WDTLAR
2   Attn: WDTVR

Chief, DASA
The Pentagon
Washington, D. C.
1   Attn: Document Library

Commanding General
Arnold Engineering Dev. Center
Tullahoma, Tenn.
1   Attn: Technical Library
5   Attn: AEKS

Commanding Officer, DOFL
Washington 25, D. C.
1   Attn: Library
             Rm. 211, Bldg. 92

NASA
George C. Marshall
Space Flight Center
Huntsville, Alabama
5   Attn: M-S&M-PT
             (Mr. H. A. Connell)
1   Attn: Dr. W. R. Lucas
             (M-SFM-M)
1   Attn: Dr. Ernst Geissler

Office, Chief of Ordnance
Department of the Army
Washington 25, D. C.
1   Attn: ORDTU

APL/JHU
8621 Georgia Avenue
Silver Spring, Md.
2   Attn: Tech. Reports Group
1   Attn: Dr. D. Fox
1   Attn: Dr. F. Hill
1   Attn: Dr. L. L. Cronvich
1   Attn: Librarian
             Via: INSORD

AVCO Manufacturing Corp.
Research & Advanced
Development Division
201 Lowell Street
Wilmington, Mass.
1   Attn: Mr. J. P. Wamser

AVCO Manufacturing Corp.
Everett, Mass.
1   Attn: Dr. Kantrowitz

General Electric Co.
Space Vehicle & Missiles Dept.
21 South 12th St.
Philadelphia, Penn.
1   Attn: Dr. J. Stewart
1   Attn: Dr. Otto Klima
1   Attn: Mr. E. J. Nolan
1   Attn: Mr. L. McCreight

General Electric Research Lab.
3198 Chestnut St.
Philadelphia, Penn.
1   Attn: Dr. Leo Steg

5   National Aeronautics and
Space Administration
1520 H Street N. W.
Washington, D. C.

NASA
High Speed Flight
Edwards Field, California
1   Attn: W. C. Williams

AERODYNAMICS DEPARTMENT
EXTERNAL DISTRIBUTION LIST (SP)

No. of
Copies

No. of
Copies

Aerospace Corporation
El Segundo, California
1   Attn: Dr. Bitondo

Lockheed Aircraft Corp.
Missiles and Space Div.
Sunnyvale, California
1   Attn: Dr. L. H. Wilson
        Via: BUWEPSREP,
        Sunnyvale, Calif.

Lockheed Aircraft Corp.
Research Lab.
Palo Alto, California
1   Attn: W. Griffith
        Via: BUWEPSREP,
        Sunnyvale, Calif.

Bureau of Naval Weapons
Representative
P. O. Box 504
Sunnyvale, California
1   Attn: SpL-314

Atomic Energy Commission
Engineering Development Br.
Division of Reactor Develop.
Headquarters, US AEC
Washington 25, D. C.
1   Attn: Mr. J. M. Simmons
1   Attn: Mr. M. J. Whitman
1   Attn: Mr. J. Conners

Lawrence Radiation Laboratory
P. O. Box 808
Livermore, California
1   Attn: Mr. W. M. Wells
        Propulsion Div.
1   Attn: Mr. Carl Kline

Oak Ridge National Laboratory
P. O. Box E
Oak Ridge, Tenn.
1   Attn: Mr. W. D. Manly

Polytechnic Institute of
Brooklyn
527 Atlantic Avenue
Freeport, N. Y.
1   Attn: Dr. Paul A. Libby
        Via: Commanding
        Officer, Office of
        Naval Res. Br. Office
        346 Broadway
        New York 13, N. Y.

Sandia Corporation
Sandia Base
Albuquerque, New Mexico
1   Attn: Mr. Alan Pope

1 Defense Metals Inf. Center
Battelle Memorial Institute
505 King Avenue
Columbus 1, Ohio

Commanding General
Army Rocket and Guided
Missile Agency
Redstone Arsenal, Alabama
1   Attn: John Morrow

National Bureau of Standards
Washington 25, D. C.
1   Attn: Dr. G. B. Schubauer

Cornell Aero. Laboratory
4455 Genesee Street
Buffalo, N. Y.
1   Attn: Dr. Gordon Hall

General Applied Sciences
Laboratories, Inc.
Merrick and Stewart Avenues
East Meadow, New York
1   Attn: Mr. Robert Byrne

Jet Propulsion Laboratory
4800 Oak Grove Drive
Pasadena 3, California
1   Attn: I. R. Kowlan, Chief
        Reports Group
2   Attn: Dr. L. Jaffee

AERODYNAMICS DEPARTMENT
EXTERNAL DISTRIBUTION LIST (SP)

No. of
Copies

Los Alamos Scientific Lab.
P. O. Box 1663
Los Alamos, New Mexico
1   Attn: Dr. D. F. MacMillan
          N-1 Group Leader

Institute for Defense Analyses
Advanced Research Projects Agency
Washington 25, D. C.
1   Attn: Mr. W. G. May
          General Sciences Branch

Kaman Aircraft Corporation
Nuclear Division
Colorado Springs, Colorado
1   Attn: Dr. A. P. Bridges

U. S. Atomic Energy Commission
P. O. Box 62
Oak Ridge, Tenn.
1   Attn: TRI:NLP:ATD:10-7

1 Sandia Corporation
Livermore Laboratory
P. O. Box 969
Livermore, California

United Aircraft Corporation
Research Laboratories
East Hartford 8, Conn.
1   Attn: Mr. H. J. Charette
1   Attn: Mr. H. Taylor

Naval Ordnance Laboratory, White Oak, Md.
(NOL technical report 61-25)
HEAT TRANSFER IN DISSOCIATED AIR BY A TWO—
THICKNESS INTEGRAL METHOD. PART II. THE
ZERO PRESSURE GRADIENT LAMINAR BOUNDARY
LAYER (U), by John O. Powers and Edgar
Krahn. 15 Dec. 1961. 19p. charts, tables.
(Aeroballistics research report 149). Tasks
NOL 363 and NOL F009-10-001 RMGA-53-401.
UNCLASSIFIED

The two-thickness integral method of de-
termining boundary-layer characteristics has
previously been shown to provide reasonable
results for stagnation point flows. Further
evaluation of its more general applicability
has been explored for the zero pressure
gradient case. It appears that of the pro-
file representations considered, a two-
parameter, sixth-degree velocity profile
gives the most desirable results for a flat
plate when used with the present method.

1. Boundary layer,
   Laminar
2. Bodies —
   Boundary layer
3. Heat —
   Transference
4. Bodies — Heat
   transfer
I. Title
II. Powers, John
   O.
III. Krahn, Edgar,
   jt. author
IV. Series
V. Project
VI. Project

Naval Ordnance Laboratory, White Oak, Md.
(NOL technical report 61-25)
HEAT TRANSFER IN DISSOCIATED AIR BY A TWO—
THICKNESS INTEGRAL METHOD. PART II. THE
ZERO PRESSURE GRADIENT LAMINAR BOUNDARY
LAYER (U), by John O. Powers and Edgar
Krahn. 15 Dec. 1961. 19p. charts, tables.
(Aeroballistics research report 149). Tasks
NOL 363 and NOL F009-10-001 RMGA-53-401.
UNCLASSIFIED

The two-thickness integral method of de-
termining boundary-layer characteristics has
previously been shown to provide reasonable
results for stagnation point flows. Further
evaluation of its more general applicability
has been explored for the zero pressure
gradient case. It appears that of the pro-
file representations considered, a two-
parameter, sixth-degree velocity profile
gives the most desirable results for a flat
plate when used with the present method.

1. Boundary layer,
   Laminar
2. Bodies —
   Boundary layer
3. Heat —
   Transference
4. Bodies — Heat
   transfer
I. Title
II. Powers, John
   O.
III. Krahn, Edgar,
   jt. author
IV. Series
V. Project
VI. Project

Naval Ordnance Laboratory, White Oak, Md.
(NOL technical report 61-25)
HEAT TRANSFER IN DISSOCIATED AIR BY A TWO—
THICKNESS INTEGRAL METHOD. PART II. THE
ZERO PRESSURE GRADIENT LAMINAR BOUNDARY
LAYER (U), by John O. Powers and Edgar
Krahn. 15 Dec. 1961. 19p. charts, tables.
(Aeroballistics research report 149). Tasks
NOL 363 and NOL F009-10-001 RMGA-53-401.
UNCLASSIFIED

The two-thickness integral method of de-
termining boundary-layer characteristics has
previously been shown to provide reasonable
results for stagnation point flows. Further
evaluation of its more general applicability
has been explored for the zero pressure
gradient case. It appears that of the pro-
file representations considered, a two-
parameter, sixth-degree velocity profile
gives the most desirable results for a flat
plate when used with the present method.

1. Boundary layer,
   Laminar
2. Bodies —
   Boundary layer
3. Heat —
   Transference
4. Bodies — Heat
   transfer
I. Title
II. Powers, John
   O.
III. Krahn, Edgar,
   jt. author
IV. Series
V. Project
VI. Project

Naval Ordnance Laboratory, White Oak, Md.
(NOL technical report 61-25)
HEAT TRANSFER IN DISSOCIATED AIR BY A TWO—
THICKNESS INTEGRAL METHOD. PART II. THE
ZERO PRESSURE GRADIENT LAMINAR BOUNDARY
LAYER (U), by John O. Powers and Edgar
Krahn. 15 Dec. 1961. 19p. charts, tables.
(Aeroballistics research report 149). Tasks
NOL 363 and NOL F009-10-001 RMGA-53-401.
UNCLASSIFIED

The two-thickness integral method of de-
termining boundary-layer characteristics has
previously been shown to provide reasonable
results for stagnation point flows. Further
evaluation of its more general applicability
has been explored for the zero pressure
gradient case. It appears that of the pro-
file representations considered, a two-
parameter, sixth-degree velocity profile
gives the most desirable results for a flat
plate when used with the present method.

1. Boundary layer,
   Laminar
2. Bodies —
   Boundary layer
3. Heat —
   Transference
4. Bodies — Heat
   transfer
I. Title
II. Powers, John
   O.
III. Krahn, Edgar,
   jt. author
IV. Series
V. Project
VI. Project